Entamoeba histolytica develops resistance to complement deposition and lysis after acquisition of human complement regulatory proteins through trogocytosis

Hannah W. Miller[1], Tammie S.Y. Tam[1] and Katherine S. Ralston[1*]

[1]Department of Microbiology and Molecular Genetics, University of California, Davis, USA

[*]Address correspondence to Katherine S. Ralston, ksralston@ucdavis.edu

Running Title: Evasion of complement lysis by *Entamoeba histolytica*

ABSTRACT

Entamoeba histolytica is the cause of amoebiasis. The trophozoite (amoeba) form of this parasite is capable of invading the intestine, and can disseminate through the bloodstream to other organs. The mechanisms that allow amoebae to evade complement deposition during dissemination have not been well characterized. We previously discovered a novel complement-evasion mechanism employed by *E. histolytica*. *E. histolytica* ingests small bites of living human cells in a process termed trogocytosis. We demonstrated that amoebae were protected from lysis by human serum following trogocytosis of human cells, and that amoebae acquired and displayed human membrane proteins from the cells they ingested. Here, we aimed to define how amoebae are protected from complement lysis after performing trogocytosis. We found that amoebae were protected from complement lysis after ingestion of both human Jurkat T cells and red blood cells, and that the level of protection correlated with the amount of material ingested. Trogocytosis of human cells led to a reduction in deposition of C3b on the surface of amoebae. We asked whether display of human complement regulators is involved in amoebic protection, and found that CD59 was displayed by amoebae after trogocytosis. Deletion of a single complement regulatory protein, CD59 or CD46, from Jurkat cells was not sufficient to alter amoebic protection from lysis, suggesting that multiple, redundant complement regulators mediate amoebic protection. However, exogeneous expression of CD46 or CD55 in amoebae was sufficient to confer protection from lysis. These studies shed light on a novel strategy for immune evasion by a pathogen.

21 **IMPORTANCE**

22 *Entamoeba histolytica* is the cause of amoebiasis, a diarrheal disease of global
23 importance. While infection is often asymptomatic, the trophozoite (amoeba) form of this
24 parasite is capable of invading and ulcerating the intestine, and can disseminate through the
25 bloodstream to other organs. Understanding how *E. histolytica* evades the complement system
26 during dissemination is of great interest. Here we demonstrate for the first time that amoebae
27 that have performed trogocytosis (nibbling of human cells) resist deposition of the complement
28 protein C3b. Amoebae that have performed trogocytosis display the complement regulatory
29 protein CD59. Overall, our studies suggest that acquisition and display of multiple, redundant
30 complement regulators is involved in amoebic protection from complement lysis. These
31 findings shed light on a novel strategy for immune evasion by a pathogen. Since other parasites
32 use trogocytosis for cell killing, our findings may apply to the pathogenesis of other infections.

33 **INTRODUCTION**

34 Amoebiasis remains a disease of global importance. The 2015 Global Burden of Disease
35 Study estimated that it was responsible for 67,900 deaths worldwide that year (1). Its causative
36 agent, *Entamoeba histolytica,* is prevalent in countries with poor sanitation and is spread
37 through feces-contaminated food and water (2). In the rural area of Durango, Mexico, the
38 seroprevalence of *E. histolytica* was found to be as high as 42% (3), and a longitudinal study of
39 children living in an urban community of Dhaka, Bangladesh found that 80% were infected with
40 the parasite by two years of age (4).

41 While infection with *E. histolytica* is often asymptomatic, it can result in diarrheal
42 disease, colitis and extraintestinal abscesses (5). Following ingestion of the cyst form of the
43 parasite, excystation occurs and the trophozoite stage (amoeba) colonizes the large intestine
44 (6). Amoebae are capable of invading and ulcerating the intestine, causing tissue damage and
45 bloody diarrhea. They can also disseminate through the bloodstream to other organs, most
46 commonly the liver, where they form abscesses that are fatal if left untreated (5). The
47 mechanisms that allow amoebae to evade complement deposition during dissemination have
48 not been well characterized. Pathogenic strains of *E. histolytica* isolated from patients have
49 been shown to be more resistant to complement lysis than nonpathogenic strains (7). It has
50 also been found that the pathogenic amoeba species *E. histolytica* appears to be more resistant
51 to complement than its nonpathogenic relative *E. dispar* (8). *E. histolytica* cysteine proteases
52 can cleave complement components (9–11), and the Gal/GalNAc lectin has been described as a
53 CD59 mimicry molecule (12). However, these mechanisms alone are not sufficient to fully

54 protect amoebae from complement lysis, as trophozoites are readily lysed by human serum *in*
55 *vitro* (13).

56 We previously discovered a novel complement-evasion mechanism employed by *E.*
57 *histolytica* (13). Trogocytosis, or "cell nibbling," is present in many eukaryotes and occurs in a
58 variety of contexts (14). In *E. histolytica*, trogocytosis is a process in which amoebae ingest small
59 bites of living human cells (15). Our previous work has defined amoebic trogocytosis as both a
60 mechanism for cell killing (15), and more recently, for immune evasion (13). We demonstrated
61 that amoebae were protected from lysis by human serum following trogocytosis of human cells
62 (13), and that amoebae acquired and displayed human membrane proteins from the cells they
63 ingested (13). This work suggested a model in which amoebae incorporate proteins from
64 human cells they eat on their surface, and these proteins in turn inhibit complement lysis.

65 In the present study, we aimed to define the mechanism by which amoebae are
66 protected from complement lysis after performing trogocytosis. We found that trogocytosis of
67 human cells reduced deposition of the complement protein C3b the surface of amoebae, and
68 that amoebae were protected from complement lysis after ingestion of both human Jurkat T
69 cells and primary red blood cells. We identified the human complement regulatory protein
70 CD59 (protectin) as one of the proteins that is taken from ingested human cells and displayed
71 on the amoebic surface. Deletion of a single complement regulatory protein, CD59 or CD46,
72 from human Jurkat cells was not sufficient to alter conferred protection on amoebae. However,
73 exogeneous expression of a single complement regulator, i.e., CD46 or CD55, in amoebae was
74 sufficient to confer protection from lysis. Overall, these studies suggest that multiple,
75 redundant complement regulators are involved in amoebic protection.

76 **RESULTS**

77 **Ingestion of beads does not confer protection from complement lysis.**

78 We previously showed that protection from complement lysis occurred in amoebae that
79 had performed trogocytosis on living human cells, and that known inhibitors of trogocytosis
80 also inhibited protection from complement lysis (13). Amoebae that had performed
81 phagocytosis of dead human cells did not become protected from complement. Likewise,
82 amoebae that were capable of trogocytosis, but defective in phagocytosis, nonetheless became
83 protected from complement (13). To extend these findings, and to examine the role of
84 ingestion on protection in the absence of host proteins, we allowed amoebae to ingest
85 increasing concentrations of latex beads. Amoebae that ingested beads were no more
86 protected from lysis than control amoebae that did not perform ingestion **(Fig. 1, S1)**. Thus,
87 trogocytosis confers protection from complement lysis, but phagocytosis of dead human cells
88 or latex beads does not confer protection.

89 **Amoebic protection from complement following trogocytosis is dose-dependent.**

90 To determine if the amount of trogocytosed human cell material influenced protection,
91 or if any level of trogocytosis was protective, we allowed amoebae to ingest incrementally
92 larger amounts. Amoebae became increasingly protected from complement lysis **(Fig. 2b-c,**
93 **S2a)** after ingesting higher quantities of live Jurkat cell material **(Fig. 2a, 2g)**. Thus, acquired
94 protection from complement lysis correlates with the amount of human cell material ingested
95 through trogocytosis.

96 We next asked if protection could be conferred through trogocytosis of primary human
97 cells. During invasive infections, amoebae breach the intestinal wall and disseminate via the

98 bloodstream. Detection of amoebae containing ingested red blood cells in the stool has
99 previously been used as a diagnostic for invasive disease (16). Therefore, we asked if ingestion
100 of human red blood cells would lead to protection. Amoebae were allowed to ingest increasing
101 numbers of human red blood cells. Increased trogocytosis of red blood cells led to increased
102 protection from complement lysis **(Fig. 2d-f, 2h, S2b)**. These results support a model where the
103 level of protection from complement lysis is proportional to the amount of human cell material
104 that was ingested during trogocytosis.

105 **Amoebic trogocytosis of human cells inhibits deposition of complement C3b.**

106 It can be inferred that lysis of amoebae by human serum is due to complement activity
107 because heat-inactivated serum does not lyse amoebae (13). Here, we formally tested if
108 trogocytosis of human cells led to reduced deposition of complement on the amoebae surface.
109 Amoebae that had been co-incubated with live human cells had less death and less deposited
110 human C3b on their surface than amoebae that were incubated in the absence of Jurkat cells
111 **(Fig. 3a-b, S3)**. Furthermore, live amoebae had less deposited C3b than dead amoebae **(Fig. 3c,**
112 **3e)**. Amoebae that had been co-incubated with human cells had less deposited C3b, compared
113 to amoebae that were incubated in the absence of Jurkat cells **(Fig. 3d)**. Therefore, trogocytosis
114 of human cells prevents complement lysis of amoebae and inhibits deposition of complement
115 C3b.

116 **Amoebae acquire the complement regulatory proteins CD59 and CD46 from human cells.**

117 We hypothesized that protection from complement lysis was due to display of human
118 complement regulatory proteins. We first chose to look at acquisition of the complement
119 regulatory protein CD59 (protectin), a membrane protein that is expressed by both Jurkat cells

120 and human red blood cells (17–19). CD59 inhibits terminal components of the complement
121 cascade and formation of the membrane attack complex (17, 20–22). After amoebae had
122 performed trogocytosis, patches of CD59 were detected on the amoeba surface within five
123 minutes **(Fig. 4a)** and a larger quantity of CD59 patches were detected on the amoeba surface
124 after one hour of trogocytosis **(Fig. 4a-c)**. The patchy/punctate localization pattern was similar
125 to the localization pattern of other human proteins displayed by amoebae after trogocytosis
126 (13). Importantly, the apparent display of human membrane proteins by amoebae was not an
127 artifact of paraformaldehyde fixation, since the appearance of human membrane proteins
128 displayed by amoebae was indistinguishable, whether staining was performed before or after
129 fixation (**Fig. S4** and (13)). Since the heavy chain of the amoeba surface Gal/GalNAc lectin has
130 been implicated as a CD59 mimicry molecule (12, 23), we asked if the CD59 antibody used in
131 these assays cross-reacted with the Gal/GalNAc lectin. CD59 was not detected on control
132 amoebae that had not performed trogocytosis **(Fig. 4a**), showing that the CD59 antibody did
133 not cross-react with the Gal/GalNAc lectin.

134 Imaging flow cytometry analysis was used to quantify amoebic acquisition of CD59.
135 Human cell nuclei are not ingested during trogocytosis (15). Therefore, labeling of human cell
136 nuclei was used to differentiate intact, extracellular human cells from patches of human
137 proteins displayed on amoebae. Patches of displayed human CD59 were detected on amoebae
138 that had performed trogocytosis, but not on amoebae that were incubated in the absence of
139 Jurkat cells **(Fig. 5a-c, S5)**. Amoebae had ~38% more displayed CD59 after one hour of
140 trogocytosis than after five minutes **(Fig. 5b)**. These findings indicate that amoebae acquired

141 and displayed CD59 within five minutes of trogocytosis, and the quantity of displayed CD59
142 increased over time.

143 To determine if more than one complement regulatory protein was displayed by
144 amoebae after trogocytosis, immunofluorescence was used to detect human CD46. CD46
145 (membrane cofactor protein) is expressed by human Jurkat cells (24) and acts as a co-factor for
146 serum factor I, which cleaves and inactivates complement components C3b and C4b (25–27).
147 After amoebae had performed trogocytosis, patches of CD46 were detected on the amoeba
148 surface within five minutes **(Fig. S6).** Thus, amoebae acquire and display multiple complement
149 regulatory proteins, after performing trogocytosis of human cells.

150 **Removal of GPI-anchored surface proteins trends towards restoring complement lysis of**
151 **amoebae.**

152 We next sought to test the effect of removing complement regulatory proteins on
153 conferred protection. CD59 is a glycosylphosphatidylinositol (GPI) anchored protein that can be
154 cleaved with the enzyme phosphatidylinositol-specific phospholipase C (PI-PLC) (17, 18, 20, 22).
155 In addition to removing CD59, treatment with PI-PLC also cleaves the GPI-anchored
156 complement regulatory protein CD55 (decay-accelerating factor) (28, 29). CD55 is expressed by
157 both Jurkat cells and human red blood cells (19, 30) and accelerates the decay of C3 and C5
158 convertases of the classical and alternative complement pathways (30, 31). Amoebae were
159 allowed to perform trogocytosis or incubated in the absence of Jurkat cells, and then treated
160 with PI-PLC before exposure to human serum. Heat-inactivated PI-PLC was used as a control. PI-
161 PLC treatment appeared to reduce amoebic protection from complement lysis **(Fig. S7, S8a)**.
162 However, this difference was not statistically significant. This is likely to be due to the higher

163 levels of variability in this assay, which were due to the prolonged incubation of amoebae on
164 ice during PI-PLC treatment. Indeed, due to the incubation on ice, the background level of
165 amoeba cell death was much higher than usual. These findings suggested that removal of all
166 GPI-anchored proteins reduces amoebic protection from complement lysis, but did not prove a
167 causal relationship.

168 **Removal of CD59 and CD46 is not sufficient to sensitize amoebae to complement lysis.**

169 Due to the higher levels of variability that we observed with PI-PLC treatment, we next
170 used human cell mutants to test whether individual proteins were required for protection from
171 complement lysis. We tested the requirements for CD59 and CD46. In order to determine if
172 acquisition and display of human CD59 or CD46 molecules was required for protection from
173 complement, we used CRISPR/Cas9 to create human cell knockout mutants that lacked these
174 proteins. Sanger sequencing **(Fig. S9)** and antibody staining of CD59 **(Fig. 6a-b)** and CD46 **(Fig.**
175 **6c-d)** showed that knockout mutants were successfully generated. Amoebae that were allowed
176 to perform trogocytosis on control human cells or cells that lacked either CD59 or CD46 were
177 equally protected from complement lysis **(Fig. 6e, S8)**. Additionally, there was no difference in
178 the amount of ingested human cell material **(Fig. 6f)**. These findings reveal that removal of
179 either CD59 or CD46 individually is not sufficient to sensitize amoebae to complement lysis.
180 Furthermore, they hint at redundancy in the mechanism of protection and that amoebae likely
181 acquire and display multiple complement regulatory proteins from the cells they ingest.

182 **Display of CD46 or CD55 is sufficient to protect amoebae from complement lysis.**

183 To ask if display of human complement regulatory proteins was sufficient to protect
184 amoebae from lysis, we created amoebae that exogenously expressed either human CD46 or

185 CD55 **(Fig. 7, S2a).** Expression of CD46 or CD55 was detectable with RT-PCR analysis **(Fig. 7a).**
186 Immunofluorescence analysis showed that CD46 or CD55 proteins were surface-localized in
187 amoebae, as they were detected with antibody staining of non-permeabilized cells **(Fig. 7b-j,**
188 **S2a).** Localization of the *E. histolytica* surface Gal/GalNAc lectin was used as a control **(Fig. 7d,**
189 **7g, 7j),** and all transfected amoebae had equivalent amounts of Gal/GalNAc lectin. CD46 or
190 CD55 expression was at a relatively low level **(Fig. 7b-c, 7e-f),** just above background
191 fluorescence of vector control amoebae. Additionally, CD46 or CD55 expression was markedly
192 lower than the expression level of the Gal/GalNAc lectin **(Fig. 7d, 7g).** When exposed to human
193 serum, amoebae that expressed human CD46 or CD55 were more protected from lysis than
194 vector control amoebae **(Fig. 8, S8b)**. Therefore, display of a single complement regulatory
195 protein is sufficient to protect amoebae from complement lysis.

196 **DISCUSSION**

197 Our findings reveal that amoebae are protected from complement lysis through
198 trogocytosis of human cells and that trogocytosis leads to less deposited C3b on the amoeba
199 surface. Amoebae acquire protection from both human Jurkat cells as well as primary red blood
200 cells and conferred protection is proportional to the amount of ingested human cell material.
201 Trogocytosis of human cells results in the display of the complement regulatory protein CD59
202 on the amoebae surface. Finally, although removal of the individual complement regulatory
203 proteins, CD59 or CD46 was not sufficient to sensitize amoebae to complement lysis, the
204 display of an individual complement regulatory protein, CD46 or CD55, was sufficient to protect
205 amoebae from complement lysis.

206 Many studies have shown that cancer cells overexpress complement regulatory
207 molecules, allowing them to evade complement lysis. However, it should be noted that
208 expression levels vary widely between cell types and between individual studies (32). Removal
209 of GPI-anchored proteins, which include the complement regulatory proteins CD59 and CD55
210 but not CD46, with PI-PLC treatment resulted in enhanced susceptibility of cancer cells to
211 complement lysis (28, 29). This is consistent with our finding that PI-PLC treated amoebae that
212 had undergone trogocytosis of human cells, and been made resistant to complement, became
213 more sensitive to complement lysis. Treatment with PI-PLC removes other GPI-anchored
214 proteins in addition to CD59 and CD55, so we cannot rule out the possibility that loss of other
215 membrane proteins contributed to the loss of complement resistance in our PI-PLC treated
216 amoebae.

217 Amoebae that were engineered to express complement regulatory proteins became
218 protected from lysis by human complement. We were unable to express human CD59 in
219 amoebae, as although stably transfected amoebae with a CD59 expression construct were
220 successfully recovered, these transfectants grew slowly and could not be maintained over time.
221 While CD59 expression was detectable by RT-PCR, it is possible that the CD59 protein mis-
222 localized in amoebae, or otherwise led to deleterious effects. CD46 and CD55 were each
223 appropriately localized to the amoeba cell surface, as evidenced by immunofluorescence
224 staining, and by the functional protection from complement lysis that they conferred. Notably,
225 CD46 and CD55 were not greatly overexpressed in amoebae. When using immunofluorescence,
226 CD46 and CD55 staining levels were just above the background levels of fluorescence seen in
227 vector control amoebae. Thus, these proteins led to protection from complement lysis without
228 dramatically high levels of expression. Only a single complement regulator at a low expression
229 level was needed for protection from lysis by complement. These findings fit with the generally
230 relatively low endogenous expression levels of complement regulatory proteins in human cells,
231 in that low levels of these proteins are sufficient to inhibit the complement pathway.
232 There have been several studies that examined the efficacy of using blocking antibodies
233 against complement regulatory proteins to enhance lysis of cancer cells. Results from blocking
234 individual proteins have been highly variable in different cell types but blocking one or more
235 proteins was effective in many cases. Using antibodies against CD46 was rarely effective,
236 however antibodies against CD59 and CD55 often were effective in enhancing complement lysis
237 (32). Additionally, there appears to be an additive effect when multiple proteins are targeted at
238 once. Cervical carcinoma cells were rendered more susceptible to complement after treatment

239 with blocking antibodies to CD59 and CD55, and lysis was increased further when cells were
240 treated with both antibodies (33). Similarly, breast carcinoma cells, were more easily lysed after
241 treatment with anti-CD59 and anti-CD55 antibodies, but a much higher degree of lysis was
242 achieved when a mixture of anti-CD59, anti-CD55, and anti-CD46 antibodies was used (34).
243 Since neither removal of CD46 or CD59 was sufficient to sensitize amoebae to complement
244 lysis, it is possible that amoebic display of multiple different complement regulators enables
245 protection from lysis. In our assays, we used a 1:40 ratio of amoebae to Jurkat cells, a ratio that
246 led to a high level of protection from complement lysis. It is possible that using fewer human
247 cells, to lead to a suboptimal level of protection from complement lysis, might have more
248 sensitively revealed differences in amoebic protection from complement lysis due to subtle
249 perturbations like the loss of individual human complement regulators. While removal of CD46
250 or CD59 did not sensitize amoebae to complement lysis, these proteins could still contribute to
251 amoebic complement protection, as part of a collection of multiple redundant, complement
252 regulators that protect amoebae from lysis. Indeed, experiments in which amoebae were
253 engineered to express complement regulators showed that display of CD46 or CD55 was
254 sufficient to protect amoebae from lysis, supporting the relevance of these proteins in
255 protecting amoebae that have performed trogocytosis.
256 Our results support a model whereby amoebae are protected from serum lysis in the
257 blood through trogocytosis of red blood cells they encounter there, and potentially from other
258 cells they encounter before reaching the bloodstream. Amoebae likely acquire and display
259 multiple complement regulatory proteins from the human cells that they ingest, which then
260 leads to less C3b deposition, and protection from complement lysis.

261 **MATERIALS AND METHODS**

262 **Cell culture**

263 *E. histolytica* trophozoites (HM1:IMSS) from ATCC (amoebae) were cultured as
264 described previously (13, 35). Amoebae were maintained in glass tissue culture tubes at 35°C in
265 TYI-S-33 medium supplemented with 15% heat-inactivated adult bovine serum (Gemini Bio-
266 Products), 2.3% Diamond vitamin Tween 80 solution (40×; Sigma-Aldrich), and 80 U/ml
267 penicillin, 80 µg/ml streptomycin (Gibco). Amoebae were expanded in T25 un-vented tissue
268 culture flasks and harvested when flasks reached 80% confluence. When used in serum lysis or
269 immunofluorescence assays, amoebae were resuspended in M199s medium (Gibco medium
270 M199 with Earle's salts, L-glutamine, and 2.2 g/liter sodium bicarbonate, without phenol red)
271 supplemented with 0.5% bovine serum albumin (BSA), 25 mM HEPES, and 5.7 mM L-cysteine.

272 Human Jurkat T cells (clone E6-1) from ATCC were grown in vented T25 tissue culture
273 flasks at 37°C and 5% CO2 as previously described (13). Jurkat cells were cultured in RPMI 1640
274 medium (Gibco; RPMI 1640 with L-glutamine and without phenol red) supplemented with 10%
275 heat-inactivated fetal bovine serum (Gibco), 100 U/ml penicillin, 100 µg/ml streptomycin, and
276 10 mM HEPES. Jurkat cells were expanded in T75 vented tissue culture flasks and harvested
277 when cell density reached between 5×10^5 and 2×10^6 cells/ml. Jurkat cells were
278 resuspended in M199s medium for use in serum lysis or immunofluorescence assays.

279 Single donor human red blood cells separated from whole blood by centrifugation and
280 negative for the presence of human immunodeficiency virus-1 (HIV-1), HIV-2, HIV-1 antigen or
281 HIV-1 nucleic acid test, hepatitis B surface antigen, hepatitis C virus , syphilis, and alanine
282 aminotransferase test were purchased from Innovative Research (Cat# IWB3CPDA1UNIT). Red

283 blood cells were stored at 4°C and resuspended in M199s medium prior to use in serum lysis
284 assays.

285 **DNA constructs**

286 For creation of Jurkat cell CRISPR knockout mutants, guide RNAs (gRNA) to human CD59
287 or CD46 were cloned into a pX330-U6-Chimeric_BB-CBh-hSpCas9 plasmid backbone (pX330-U6-
288 Chimeric_BB-CBh-hSpCas9 was a gift from Feng Zhang (Addgene plasmid # 42230;
289 http://n2t.net/addgene:42230 ; RRID:Addgene_42230) (36)). Guide RNAs were created by using
290 the sequences designed by Thielen et. al, 2018 (37). The gRNA oligos used are presented in
291 Table 1 with BbsI restriction enzyme overhangs shown in bold. Guide RNAs were cloned into
292 the pX330-U6-Chimeric_BB-CBh-hSpCas9 plasmid backbone using a modified version of the
293 Zhang Lab General Cloning Protocol (Addgene http://www.addgene.org/crispr/zhang/). Briefly,
294 the px330 plasmid backbone was digested with BbsI restriction enzyme (FastDigest BpiI:
295 ThermoFisher Scientific). Guide RNA oligos containing BbsI overhangs were then
296 phosphorylated and annealed. Next, annealed oligos were ligated into the pX330 plasmid
297 backbone and NEB 5-alpha Competent *E. coli* were transformed (New England Biolabs). Positive
298 colonies were screened by restriction digest. Plasmids with the correct inserts were confirmed
299 by Sanger sequencing using the "U6" Universal Primer from GENEWIZ (LKO.1 5') which is
300 located in the human U6 promoter **(Table 1)**.

301 To generate amoebic expression constructs for exogeneous expression of human
302 proteins, the coding regions of human CD46 or CD55 were amplified from human Jurkat cells.
303 Briefly, RNA was extract from Jurat cells using the Direct-zol RNA MiniPrep Plus kit (Zymo
304 Research) and cDNA was prepared. Next, the coding sequences for human CD46 or CD55 were

305 amplified from Jurkat cDNA by PCR using primers described in **Table 1.** The amplified CD46 or
306 CD55 inserts were then cloned into the *E. histolytica* expression plasmid pEhEx backbone (38)
307 using the Gibson Assembly Ultra Kit (VWR). Primers used for Gibson cloning are described in
308 **Table 1.** For creation of the CD46 expression plasmid, both the pEhEx backbone and the CD46
309 insert were PCR amplified with primers that added 20 base pairs corresponding to the ends of
310 the insert or backbone, respectively. For creation of the CD55 expression plasmid, the pEhEx
311 backbone was digested using XhoI (New England Biolabs) and the CD55 insert was PCR
312 amplified with primers that added 20 base pairs corresponding to the ends of the backbone.
313 NEB 5-alpha Competent *E. coli* were transformed, and positive colonies were screened by
314 restriction digest analysis. Sanger sequencing was used to assess the sequences of the inserts
315 and flanking vector sequences, using primers located in the Cysteine synthase A gene
316 [EHI_024230] 5' and 3' UTR regions **(Table 1)**. The CD46 gene insert corresponds to the mRNA
317 transcript variant d (GenBank accession number: NM_153826) and the CD55 gene insert
318 corresponds to mRNA transcript variant 1 (GenBank accession number: NM_000574).

319 **Jurkat T cell CRISPR/Cas9 mutants**

320 Human Jurkat T cells were transfected with pX330 plasmids containing the CD59 gRNA,
321 the CD46 gRNA, or the pX330 backbone as a control. Plasmid DNA was isolated in an endotoxin-
322 free manner (GenElute™ HP Endotoxin-Free Plasmid Maxiprep Kit; Sigma-Aldrich) and
323 concentrated using paramagnetic beads (HighPrep PCR Clean Up System; Magbio). Jurkat T cells
324 were transfected using the Neon Transfection System (Invitrogen) with the 10 µl tip and 24 well
325 plate format. Cells were prepared, and the Neon Transfection System was used according to

326 the manufacturer's instructions. The transfection conditions used were as follows: volts = 1050,
327 width = 30 and pulse # = 2.

328 When creating the CD59 and CD46 knockout mutants, 1.8 µg of plasmid DNA was used
329 with 1 x 10^5 cells per transfection reaction and two reactions were performed for each plasmid
330 and transferred to 1 well of a 24 well plate. Transfection efficiency was calculated by separately
331 transfecting an enhanced green fluorescent protein (EGFP) expression plasmid pcDNA3-EGFP
332 (pcDNA3-EGFP was a gift from Doug Golenbock (Addgene plasmid # 13031 ;
333 http://n2t.net/addgene:13031 ; RRID:Addgene_13031)) in parallel. Percentage of EGFP
334 expressing cells was calculated after 24 hours by fixing samples with 4% paraformaldehyde
335 (Electron Microscopy Sciences) and analyzing with imaging flow cytometry. To generate CD59
336 expressing Jurkat cells, 2 µg of plasmid DNA was used with 2 x 10^5 cells per transfection reaction
337 and two reactions were performed for each plasmid and transferred to 1 well of a 24 well plate.

338 Clonal lines of Jurkat cell mutants were obtained by limiting dilution in 96 well plates.
339 Clonal lines were screened for knockout by labeling with primary mouse monoclonal antibodies
340 to CD59 (clone MEM-43/5; Abcam) or CD46 (clone C-10; Santa Cruz Biotechnology) and a Cy™5
341 AffiniPure Goat Anti-Mouse secondary antibody (Jackson ImmunoResearch Laboratories, Inc).
342 Samples were analyzed by imaging flow cytometry. Knockout was confirmed in positive clones
343 by isolating genomic DNA using the Quick-DNA Miniprep kit (Zymo Research) and polymerase
344 chain reaction (PCR) amplifying regions of either CD59 or CD46. Primer sets had been identified
345 in BLAST as specific to these genes **(Table 1)**. Next, purified PCR product was sequenced with
346 primers upstream of the predicted CRISPR/Cas9 cut site **(Table 1)** and knockout was confirmed.

347 **Characterization of amoebae exogenously expressing human CD46 or CD55**

348 Amoebae were transfected as described previously (13). Briefly, amoebae were
349 transfected with 20 µg of the human CD46 or CD55 expression construct, or the pEhEx plasmid
350 backbone using Attractene transfection reagent (Qiagen). Stable transfectants were initially
351 selected at 3 µg/ml Geneticin (ThermoFisher Scientific), and then maintained at 6 µg/ml
352 Geneticin. Before use in immunofluorescence assays and serum lysis experiments, drug
353 selection was gradually increased from 6 µg/ml to 48 µg/ml Geneticin, to increase plasmid copy
354 number. Amoebae were maintained at 48 µg/ml Geneticin for 24 hours before experiments
355 were performed.

356 Expression of human CD46 and CD55 was confirmed using RT-PCR analysis of amoebae
357 maintained at 3 µg/ml Geneticin. RNA was extracted using the Direct-zol RNA MiniPrep Plus kit
358 (Zymo Research) and cDNA was made. Primers used for RT-PCR are shown in Table 1. RT-PCR
359 was performed as described (35).

360 **Imaging flow cytometry**

361 To detect human CD59 displayed on amoebae following trogocytosis, Jurkat cells were
362 with labeled Hoechst 33342 dye (Invitrogen) at 5 µg/ml for 30 minutes at 37°C. Amoebae were
363 washed and resuspended in M199s medium and labeled with CellTracker green 5-
364 chloromethylfluorescein diacetate (CMFDA; Invitrogen) at 186 ng/ml for 10 minutes at 35°C.
365 Amoebae and Jurkat cells were then washed and resuspended in M199s medium. Amoebae
366 were resuspended at 4 x 10^5 cells/ml and Jurkat cells were resuspended at 1.6 x 10^7 cells/ ml for
367 a 1:40 amoeba: Jurkat cell ratio. Amoebae and Jurkat cells were co-incubated for either 5
368 minutes or 1 hour, or amoebae were incubated in the absence of Jurkat cells. Cells were fixed
369 with 4% PFA for 30 minutes at room temperature. Samples were blocked in 1 x PBS containing

370 0.1% Tween20 (Sigma-Aldrich) (1 x PBST), 5% BSA and 20% Normal Goat Serum (Jackson
371 ImmunoResearch Laboratories, Inc) for 1 hour at room temperature on a rocker. Next, samples
372 were labeled with primary mouse monoclonal antibodies to CD59 (clone MEM-43/5; Abcam)
373 diluted 1:50 in blocking solution at 4°C overnight on a rocker. Samples were washed with 1 x
374 PBST and labeled with a Cy5 AffiniPure Goat Anti-Mouse secondary antibody (Jackson
375 ImmunoResearch Laboratories, Inc) stored in 50% glycerol (Sigma-Aldrich). The secondary
376 antibody was diluted 1:100 in blocking solution, for a final dilution of 1:200, and incubated for 3
377 hours at room temperature on a rocker. Lastly, samples were washed with 1 x PBST,
378 resuspended in 50 µl 1 x PBS, and run on an Amnis ImageStreamX Mark II. 10,000 events were
379 collected for conditions where amoebae were incubated in the absence of Jurkat cells and
380 100,000 events were collected for conditions where amoebae were incubated with Jurkat cells.
381 Data are from 5 replicates across 3 independent experiments. The no primary control condition
382 was performed in 2 of 3 independent experiments and data are from 3 replicates. See Figure S5
383 for the analysis gating scheme.
384 To detect human CD46 displayed on amoebae following trogocytosis, amoebae and
385 Jurkat cells were labeled in the same manner as for detection of CD59. Amoebae and Jurkat
386 cells were co-incubated for 5 minutes or amoebae were incubated in the absence of Jurkat
387 cells. Samples were labeled with a primary mouse monoclonal antibody to human CD46 (Clone
388 C-10; Santa Cruz Biotechnology) at a 1:10 dilution, followed by a Cy5 AffiniPure Goat Anti-
389 Mouse secondary antibody (Jackson ImmunoResearch Laboratories, Inc). Amoebae were gated
390 on by size and 10,000 events were collected per sample. Data are from 2 replicates and 1
391 independent experiment.

392 For detection of CD46, CD55, or Gal/GalNAc lectin expression on amoebae exogenously
393 expressing CD46 or CD55, amoebae were labeled with CMFDA and prepared in the same
394 manner as for detection of displayed human CD59. Following fixation, samples were blocked
395 overnight at 4°C on a rocker. Samples were then labeled with primary mouse monoclonal
396 antibodies to human CD46 (Clone C-10; Santa Cruz Biotechnology) human CD55 (Clone NaM16-
397 4D3; Santa Cruz Biotechnology) or the *E. histolytica* Gal/GalNAc lectin (Clone 7F4; the
398 Gal/GalNAc lectin antibody was a gift from William A. Petri, Jr., University of Virginia (39))
399 overnight at 4°C on a rocker. The CD46 and CD55 primary antibodies were diluted 1:10 and the
400 Gal/GalNAc lectin primary antibody was diluted 1:50 in blocking solution. Samples were labeled
401 with secondary antibody as described above. Amoebae were gated on by size and 10,000
402 events were collect per sample. Data are from 3-4 replicates from 2 independent experiments.
403 See Figure S2a for the analysis gating scheme.

404 **Confocal microscopy**

405 To detect displayed CD59 on the amoeba surface after trogocytosis, cells were labeled
406 for confocal microscopy as described previously (13). Amoebae were prepared in the same
407 manner as the for the detection of displayed CD59 using imaging flow cytometry (above) with
408 an approximate fourfold increased concentration of CMFDA. After labeling with antibodies,
409 samples were mounted using Vectashield (Vector Laboratories) on Superfrost Plus microslides
410 (VWR) with glass coverslips. Slides were imaged on an Intelligent Imaging Innovations hybrid
411 Spinning Disk Confocal-TIRF-Widefield Microscope. 136 Images were collected from 1
412 independent experiment. FIJI software was used for image analysis (40).

413 For detection of displayed biotinylated human cell membrane proteins, amoebae were
414 left unstained in some experiments or labeled with CMFDA as described above. Human Jurkat
415 cells were biotinylated as described previously (13). Briefly, Jurkat cells were biotinylated with
416 EZ-Link Sulfo-NHS-SS-Biotin (ThermoFisher Scientific) at 480 µg/ml in 1× PBS for 25 min at 4°C.
417 The reaction was quenched using 100 mM Tris-HCl (pH 8) and washed with washed in 100 mM
418 Tris-HCl (pH 8) before being resuspending M199s medium. Amoebae were incubated with
419 biotinylated Jurkat cells at a 1:5 ratio for 2 - 5 minutes and then immediately placed on ice.
420 Next, samples were stained with Alexa Fluor 633 conjugated streptavidin (Invitrogen) at
421 20 µg/ml for 1 hour at 4°C, prior to fixation with 4% paraformaldehyde for 30 minutes at room
422 temperature. In some experiments, samples were labeled with DAPI (4 ,6-diamidino-2-
423 phenylindole; Sigma-Aldrich) for 10 minutes at room temperature following fixation. Samples
424 were mounted on either poly-lysine (Sigma-Aldrich) or collagen (collagen I, rat tail; Gibco)
425 coated coverslips for 1 hour. Samples were mounted with Vectashield on glass slides, and slides
426 were imaged on an Olympus FV1000 laser point-scanning confocal microscope.

427 **Serum lysis assays**

428 For experiments where amoebae were incubated with increasing numbers of Jurkat
429 cells, amoebae were washed and resuspended in M199s medium and labeled with CMFDA at
430 186 ng/ml for 10 minutes at 35°C. Jurkat cells were washed and labeled in M199s with DiD at
431 21 µg/ml for 5 minutes at 37°C and 10 minutes at 4°C. Amoebae were washed and
432 resuspended at 4 x 10^5 cells/ml. Jurkat cells were washed a resuspended at 2 x 10^6 cells/ml, 4 x
433 10^6 cells/ml, 8 x 10^6 cells/ml and 1.6 x 10^7 cells/ml. Amoebae were incubated in the absence of
434 Jurkat cells or the presence of Jurkat cells at a 1:5, 1:10, 1:20, and 1:40 ratio for 1 hour at 35°C.

435 Next, samples were resuspended in 100% normal human serum (pooled normal human
436 complement serum; Innovative Research Inc.) supplemented with 150 µM $CaCl_2$ and 150 µM
437 $MgCl_2$ for 30 minutes at 35°C as described previously (13). Following exposure to human serum,
438 samples were resuspended in M199s medium and labeled using Zombie Violet Fixable Viability
439 dye (BioLegend), prepared according to the manufacturer's instructions, at a concentration of
440 4 µl/ml for 30 minutes on ice. Next, samples were fixed with 4% PFA at room temperature for
441 30 minutes. Samples were then resuspended in 50 µl 1 x PBS, and run on an Amnis
442 ImageStreamX Mark II. 10,000 events were collected for samples where amoebae were
443 incubated in the absence of Jurkat cells or with Jurkat cells at a 1:5 ratio. 10,00 – 20,000 events
444 were collected for samples with Jurkat cells at a 1:10 ratio, 10,00 - 40,000 events were collected
445 for samples with a 1:20 ratio, and 50,000 - 80,000 events for samples with a 1:40 ratio. Data are
446 from 6 replicates across 3 independent experiments. See Figure S2 for the analysis gating
447 scheme.
448 For experiments with CD59 and CD46 knockout mutants, the serum lysis assay used was
449 the same as described above, except only a 1:40 ratio of amoebae to Jurkat cells was used,
450 instead of multiple different ratios. Amoebae were incubated in the absence of Jurkat cells, in
451 the presence of Jurkat cells transfected with the px330 vector control, or with either CD59 or
452 CD46 knockout Jurkat cell mutants at a 1:40 ratio. Cells were gated on by size and 10,000
453 events from the amoebae that were incubated in the absence of Jurkat cells and 100,000
454 events from the amoebae incubated with Jurkat cells were collected. Data are from 6 replicates
455 across 3 independent experiments. See Figure S8a for the analysis gating scheme.

456 In experiments where samples were treated with phospholipase C, the assay was
457 performed as described above with the addition of a treatment step preceding exposure to
458 serum. Only a 1:40 ratio of amoebae to Jurkat cells was used, instead of multiple different
459 ratios. Following coincubation of amoebae and Jurkat cells, samples were immediately placed
460 on ice and resuspended in ice-cold M199s medium. Samples were treated with either 500 mU
461 of Phospholipase C (PI-PLC) (Phospholipase C, Phosphatidylinositol-specific from *Bacillus cereus*;
462 Sigma-Aldrich) prepared according to the manufacturer's instructions, or 500 mU heat-
463 inactivated PI-PLC. PI-PLC was heat-inactivated at 95°C for 30 minutes. PI-PLC was carried out
464 on ice, on a rocker, in a 4°C cold room for 30 minutes. Cells were gated on by size and 10,000
465 events from the amoebae incubated in the absence of Jurkat cells and 100,000 events from the
466 amoebae incubated with Jurkat cells were collected. Data are from 8 replicates across 4
467 independent experiments. The untreated control condition was performed 3 of 4 independent
468 experiments and data are from 6 replicates. See Figure S8a for the analysis gating scheme.
469 For experiments where amoebae were incubated with increasing numbers of red blood
470 cells, amoebae were incubated with red blood cells resuspended at 4×10^6 cells/ml, 4×10^7
471 cells/ml, and 4×10^8 cells/ml for a 1:10, 1:100, and 1:1000 amoebae to red blood cell ratio. The
472 amoeba population was gated on by size and 10,000 amoeba events were collected for
473 samples where amoebae were incubated in the absence of red blood cells or with red blood
474 cells at a 1:10 ratio, a 1:100 ratio. 100,000 events were collected for amoebae incubated with
475 red blood cells at a 1:1000 ratio. Data are from 6 replicates from 3 independent experiments.
476 See Figure S2b for the analysis gating scheme.

477 For C3b experiments, amoebae were labeled with CMFDA and Jurkat cells were left
478 unlabeled. Amoebae and Jurkats were incubated together at a 1:40 amoebae: Jurkat ratio.
479 After fixation, samples were blocked in 1 x PBST containing 5% BSA and 20% Normal Goat
480 Serum for 30 minutes at room temperature on a rocker. Samples were then labeled with a
481 mouse monoclonal antibody to complement components C3b and iC3b (Clone 3E7; Sigma-
482 Aldrich) diluted 1:100 in blocking solution at 4°C overnight on a rocker. Samples were washed in
483 1 x PBST and labeled with an Alexa Fluor 47 AffiniPure Fab Fragment Donkey Anti-Mouse
484 secondary antibody (Jackson ImmunoResearch Laboratories, Inc) stored in 50% glycerol (Sigma-
485 Aldrich). The secondary antibody was diluted 1:100 in blocking solution for a final dilution of
486 1:200, and samples were incubated for 3 hours at room temperature on a rocker. Samples were
487 washed in 1 x PBST, resuspended in 50 µl 1 x PBS, and run on an Amnis ImageStreamX Mark II.
488 10,000 events were collected in samples where amoebae were incubated in the absence of
489 Jurkat cells and 100,000 events were collected in samples where amoebae were incubated with
490 Jurkat cells. Data are from 6 replicates across 3 independent experiments. See Figure S3 for the
491 analysis gating scheme.
492 For latex bead ingestion experiments, amoebae were left unstained and incubated with
493 either $3x10^6$ or $1.5x10^7$ fluorescent red carboxylate-modified polystyrene 2.0 µm latex beads
494 (Sigma-Aldrich) or incubated in the absence of latex beads. Amoebae were gated on by size and
495 10,000 events were collected per sample. Data are from 4 replicates across 2 independent
496 experiments. See Figure S1 for the gating scheme used for analysis.
497 For experiments with amoebae exogenously expressing human CD46 or CD55, amoebae
498 or vector control amoebae were labeled with CMFDA. Amoebae were either treated with

499 M199s medium or exposed to human serum as described above. After gating on amoebae by

500 size, 10,000 events were collected per sample. Data are from 8 replicates across 4 independent

501 experiments. See Figure S8b for the gating scheme used for analysis.

502 **Statistical analysis**

503 GraphPad Prism software was used to perform all statistical analyses and the means and

504 standard deviation values are displayed on all data plots. Analyses were done using a Student's

505 unpaired t test (no significant difference was indicated by a P of >0.05; *, P ≤ 0.05; **,

506 P ≤ 0.01; ***, P ≤ 0.001; ****, P ≤ 0.0001).

507 **ACKNOWLEDGMENTS**

508 We thank Dr. Scott Dawson, Dr. Stephen McSorley, and the members of our laboratory
509 for helpful discussions. All ImageStream and confocal data were acquired using shared
510 instrumentation in the UC Davis MCB Light Microscopy Imaging Facility. We thank Dr. Michael
511 Paddy for technical support in the use of these instruments. T.S.Y.T. was funded by the Khaira
512 Family Experiential Learning Award through the UC Davis College of Biological Sciences. This
513 work was funded by NIH grant AI146914 and a Pew Scholarship awarded to K.S.R.

514 **AUTHOR CONTRIBUTIONS**

515 H.W.M. designed, performed, and analyzed the experiments. T.S.Y.T. created and
516 characterized amoebae exogenously expressing complement regulatory proteins. K.S.R.
517 conceived of the overall approach and oversaw the design and analysis of the experiments.
518 H.W.M. and K.S.R. wrote the manuscript.

519 **REFERENCES**

520 1. Wang H, Naghavi M, Allen C, Barber RM, Bhutta ZA, Carter A, Casey DC, Charlson FJ, Chen
521 AZ, Coates MM, Coggeshall M, Dandona L, Dicker DJ, Erskine HE, Ferrari AJ, Fitzmaurice C,
522 Foreman K, Forouzanfar MH, Fraser MS, Fullman N, Gething PW, Goldberg EM, Graetz N,
523 Haagsma JA, Hay SI, Huynh C, Johnson CO, Kassebaum NJ, Kinfu Y, Kulikoff XR, Kutz M, Kyu
524 HH, Larson HJ, Leung J, Liang X, Lim SS, Lind M, Lozano R, Marquez N, Mensah GA, Mikesell
525 J, Mokdad AH, Mooney MD, Nguyen G, Nsoesie E, Pigott DM, Pinho C, Roth GA, Salomon JA,
526 Sandar L, Silpakit N, Sligar A, Sorensen RJD, Stanaway J, Steiner C, Teeple S, Thomas BA,
527 Troeger C, VanderZanden A, Vollset SE, Wanga V, Whiteford HA, Wolock T, Zoeckler L,
528 Abate KH, Abbafati C, Abbas KM, Abd-Allah F, Abera SF, Abreu DMX, Abu-Raddad LJ, Abyu
529 GY, Achoki T, Adelekan AL, Ademi Z, Adou AK, Adsuar JC, Afanvi KA, Afshin A, Agardh EE,
530 Agarwal A, Agrawal A, Kiadaliri AA, Ajala ON, Akanda AS, Akinyemi RO, Akinyemiju TF,
531 Akseer N, Lami FHA, Alabed S, Al-Aly Z, Alam K, Alam NKM, Alasfoor D, Aldhahri SF, Aldridge
532 RW, Alegretti MA, Aleman AV, Alemu ZA, Alexander LT, Alhabib S, Ali R, Alkerwi A, Alla F,
533 Allebeck P, Al-Raddadi R, Alsharif U, Altirkawi KA, Martin EA, Alvis-Guzman N, Amare AT,
534 Amegah AK, Ameh EA, Amini H, Ammar W, Amrock SM, Andersen HH, Anderson BO,
535 Anderson GM, Antonio CAT, Aregay AF, Ärnlöv J, Arsenijevic VSA, Artaman A, Asayesh H,
536 Asghar RJ, Atique S, Avokpaho EFGA, Awasthi A, Azzopardi P, Bacha U, Badawi A, Bahit MC,
537 Balakrishnan K, Banerjee A, Barac A, Barker-Collo SL, Bärnighausen T, Barregard L, Barrero
538 LH, Basu A, Basu S, Bayou YT, Bazargan-Hejazi S, Beardsley J, Bedi N, Beghi E, Belay HA, Bell
539 B, Bell ML, Bello AK, Bennett DA, Bensenor IM, Berhane A, Bernabé E, Betsu BD, Beyene AS,
540 Bhala N, Bhalla A, Biadgilign S, Bikbov B, Abdulhak AAB, Biroscak BJ, Biryukov S, Bjertness E,

541 Blore JD, Blosser CD, Bohensky MA, Borschmann R, Bose D, Bourne RRA, Brainin M, Brayne
542 CEG, Brazinova A, Breitborde NJK, Brenner H, Brewer JD, Brown A, Brown J, Brugha TS,
543 Buckle GC, Butt ZA, Calabria B, Campos-Nonato IR, Campuzano JC, Carapetis JR, Cárdenas R,
544 Carpenter DO, Carrero JJ, Castañeda-Orjuela CA, Rivas JC, Catalá-López F, Cavalleri F, Cercy
545 K, Cerda J, Chen W, Chew A, Chiang PP-C, Chibalabala M, Chibueze CE, Chimed-Ochir O,
546 Chisumpa VH, Choi J-YJ, Chowdhury R, Christensen H, Christopher DJ, Ciobanu LG, Cirillo M,
547 Cohen AJ, Colistro V, Colomar M, Colquhoun SM, Cooper C, Cooper LT, Cortinovis M, Cowie
548 BC, Crump JA, Damsere-Derry J, Danawi H, Dandona R, Daoud F, Darby SC, Dargan PI, das
549 Neves J, Davey G, Davis AC, Davitoiu DV, de Castro EF, de Jager P, Leo DD, Degenhardt L,
550 Dellavalle RP, Deribe K, Deribew A, Dharmaratne SD, Dhillon PK, Diaz-Torné C, Ding EL, dos
551 Santos KPB, Dossou E, Driscoll TR, Duan L, Dubey M, Duncan BB, Ellenbogen RG, Ellingsen
552 CL, Elyazar I, Endries AY, Ermakov SP, Eshrati B, Esteghamati A, Estep K, Faghmous IDA,
553 Fahimi S, Faraon EJA, Farid TA, Farinha CS e S, Faro A, Farvid MS, Farzadfar F, Feigin VL,
554 Fereshtehnejad S-M, Fernandes JG, Fernandes JC, Fischer F, Fitchett JRA, Flaxman A, Foigt
555 N, Fowkes FGR, Franca EB, Franklin RC, Friedman J, Frostad J, Fürst T, Futran ND, Gall SL,
556 Gambashidze K, Gamkrelidze A, Ganguly P, Gankpé FG, Gebre T, Gebrehiwot TT,
557 Gebremedhin AT, Gebru AA, Geleijnse JM, Gessner BD, Ghoshal AG, Gibney KB, Gillum RF,
558 Gilmour S, Giref AZ, Giroud M, Gishu MD, Giussani G, Glaser E, Godwin WW, Gomez-Dantes
559 H, Gona P, Goodridge A, Gopalani SV, Gosselin RA, Gotay CC, Goto A, Gouda HN, Greaves F,
560 Gugnani HC, Gupta R, Gupta R, Gupta V, Gutiérrez RA, Hafezi-Nejad N, Haile D, Hailu AD,
561 Hailu GB, Halasa YA, Hamadeh RR, Hamidi S, Hancock J, Handal AJ, Hankey GJ, Hao Y, Harb
562 HL, Harikrishnan S, Haro JM, Havmoeller R, Heckbert SR, Heredia-Pi IB, Heydarpour P,

563 Hilderink HBM, Hoek HW, Hogg RS, Horino M, Horita N, Hosgood HD, Hotez PJ, Hoy DG,
564 Hsairi M, Htet AS, Htike MMT, Hu G, Huang C, Huang H, Huiart L, Husseini A, Huybrechts I,
565 Huynh G, Iburg KM, Innos K, Inoue M, Iyer VJ, Jacobs TA, Jacobsen KH, Jahanmehr N,
566 Jakovljevic MB, James P, Javanbakht M, Jayaraman SP, Jayatilleke AU, Jeemon P, Jensen PN,
567 Jha V, Jiang G, Jiang Y, Jibat T, Jimenez-Corona A, Jonas JB, Joshi TK, Kabir Z, Kamal R, Kan H,
568 Kant S, Karch A, Karema CK, Karimkhani C, Karletsos D, Karthikeyan G, Kasaeian A, Katibeh
569 M, Kaul A, Kawakami N, Kayibanda JF, Keiyoro PN, Kemmer L, Kemp AH, Kengne AP, Keren
570 A, Kereselidze M, Kesavachandran CN, Khader YS, Khalil IA, Khan AR, Khan EA, Khang Y-H,
571 Khera S, Khoja TAM, Kieling C, Kim D, Kim YJ, Kissela BM, Kissoon N, Knibbs LD, Knudsen AK,
572 Kokubo Y, Kolte D, Kopec JA, Kosen S, Koul PA, Koyanagi A, Krog NH, Defo BK, Bicer BK,
573 Kudom AA, Kuipers EJ, Kulkarni VS, Kumar GA, Kwan GF, Lal A, Lal DK, Lalloo R, Lallukka T,
574 Lam H, Lam JO, Langan SM, Lansingh VC, Larsson A, Laryea DO, Latif AA, Lawrynowicz AEB,
575 Leigh J, Levi M, Li Y, Lindsay MP, Lipshultz SE, Liu PY, Liu S, Liu Y, Lo L-T, Logroscino G, Lotufo
576 PA, Lucas RM, Lunevicius R, Lyons RA, Ma S, Machado VMP, Mackay MT, MacLachlan JH,
577 Razek HMAE, Magdy M, Razek AE, Majdan M, Majeed A, Malekzadeh R, Manamo WAA,
578 Mandisarisa J, Mangalam S, Mapoma CC, Marcenes W, Margolis DJ, Martin GR, Martinez-
579 Raga J, Marzan MB, Masiye F, Mason-Jones AJ, Massano J, Matzopoulos R, Mayosi BM,
580 McGarvey ST, McGrath JJ, McKee M, McMahon BJ, Meaney PA, Mehari A, Mehndiratta
581 MM, Mejia-Rodriguez F, Mekonnen AB, Melaku YA, Memiah P, Memish ZA, Mendoza W,
582 Meretoja A, Meretoja TJ, Mhimbira FA, Micha R, Millear A, Miller TR, Mirarefin M,
583 Misganaw A, Mock CN, Mohammad KA, Mohammadi A, Mohammed S, Mohan V, Mola
584 GLD, Monasta L, Hernandez JCM, Montero P, Montico M, Montine TJ, Moradi-Lakeh M,

585 Morawska L, Morgan K, Mori R, Mozaffarian D, Mueller UO, Murthy GVS, Murthy S, Musa
586 KI, Nachega JB, Nagel G, Naidoo KS, Naik N, Naldi L, Nangia V, Nash D, Nejjari C, Neupane S,
587 Newton CR, Newton JN, Ng M, Ngalesoni FN, de Dieu Ngirabega J, Nguyen QL, Nisar MI,
588 Pete PMN, Nomura M, Norheim OF, Norman PE, Norrving B, Nyakarahuka L, Ogbo FA,
589 Ohkubo T, Ojelabi FA, Olivares PR, Olusanya BO, Olusanya JO, Opio JN, Oren E, Ortiz A,
590 Osman M, Ota E, Ozdemir R, Pa M, Pain A, Pandian JD, Pant PR, Papachristou C, Park E-K,
591 Park J-H, Parry CD, Parsaeian M, Caicedo AJP, Patten SB, Patton GC, Paul VK, Pearce N,
592 Pedro JM, Stokic LP, Pereira DM, Perico N, Pesudovs K, Petzold M, Phillips MR, Piel FB, Pillay
593 JD, Plass D, Platts-Mills JA, Polinder S, Pope CA, Popova S, Poulton RG, Pourmalek F,
594 Prabhakaran D, Qorbani M, Quame-Amaglo J, Quistberg DA, Rafay A, Rahimi K, Rahimi-
595 Movaghar V, Rahman M, Rahman MHU, Rahman SU, Rai RK, Rajavi Z, Rajsic S, Raju M,
596 Rakovac I, Rana SM, Ranabhat CL, Rangaswamy T, Rao P, Rao SR, Refaat AH, Rehm J,
597 Reitsma MB, Remuzzi G, Resnikoff S, Ribeiro AL, Ricci S, Blancas MJR, Roberts B, Roca A,
598 Rojas-Rueda D, Ronfani L, Roshandel G, Rothenbacher D, Roy A, Roy NK, Ruhago GM, Sagar
599 R, Saha S, Sahathevan R, Saleh MM, Sanabria JR, Sanchez-Niño MD, Sanchez-Riera L, Santos
600 IS, Sarmiento-Suarez R, Sartorius B, Satpathy M, Savic M, Sawhney M, Schaub MP, Schmidt
601 MI, Schneider IJC, Schöttker B, Schutte AE, Schwebel DC, Seedat S, Sepanlou SG, Servan-
602 Mori EE, Shackelford KA, Shaddick G, Shaheen A, Shahraz S, Shaikh MA, Shakh-Nazarova M,
603 Sharma R, She J, Sheikhbahaei S, Shen J, Shen Z, Shepard DS, Sheth KN, Shetty BP, Shi P,
604 Shibuya K, Shin M-J, Shiri R, Shiue I, Shrime MG, Sigfusdottir ID, Silberberg DH, Silva DAS,
605 Silveira DGA, Silverberg JI, Simard EP, Singh A, Singh GM, Singh JA, Singh OP, Singh PK, Singh
606 V, Soneji S, Søreide K, Soriano JB, Sposato LA, Sreeramareddy CT, Stathopoulou V, Stein DJ,

607 Stein MB, Stranges S, Stroumpoulis K, Sunguya BF, Sur P, Swaminathan S, Sykes BL, Szoeke
608 CEI, Tabarés-Seisdedos R, Tabb KM, Takahashi K, Takala JS, Talongwa RT, Tandon N,
609 Tavakkoli M, Taye B, Taylor HR, Ao BJT, Tedla BA, Tefera WM, Have MT, Terkawi AS, Tesfay
610 FH, Tessema GA, Thomson AJ, Thorne-Lyman AL, Thrift AG, Thurston GD, Tillmann T,
611 Tirschwell DL, Tonelli M, Topor-Madry R, Topouzis F, Towbin JA, Traebert J, Tran BX,
612 Truelsen T, Trujillo U, Tura AK, Tuzcu EM, Uchendu US, Ukwaja KN, Undurraga EA, Uthman
613 OA, Dingenen RV, van Donkelaar A, Vasankari T, Vasconcelos AMN, Venketasubramanian N,
614 Vidavalur R, Vijayakumar L, Villalpando S, Violante FS, Vlassov VV, Wagner JA, Wagner GR,
615 Wallin MT, Wang L, Watkins DA, Weichenthal S, Weiderpass E, Weintraub RG, Werdecker A,
616 Westerman R, White RA, Wijeratne T, Wilkinson JD, Williams HC, Wiysonge CS,
617 Woldeyohannes SM, Wolfe CDA, Won S, Wong JQ, Woolf AD, Xavier D, Xiao Q, Xu G, Yakob
618 B, Yalew AZ, Yan LL, Yano Y, Yaseri M, Ye P, Yebyo HG, Yip P, Yirsaw BD, Yonemoto N, Yonga
619 G, Younis MZ, Yu S, Zaidi Z, Zaki MES, Zannad F, Zavala DE, Zeeb H, Zeleke BM, Zhang H,
620 Zodpey S, Zonies D, Zuhlke LJ, Vos T, Lopez AD, Murray CJL. 2016. Global, regional, and
621 national life expectancy, all-cause mortality, and cause-specific mortality for 249 causes of
622 death, 1980–2015: a systematic analysis for the Global Burden of Disease Study 2015. The
623 Lancet 388:1459–1544.

624 2. Marie C, Petri WA. 2013. Amoebic dysentery. BMJ Clin Evid 2013:0918.

625 3. Alvarado-Esquivel C, Hernandez-Tinoco J, Sanchez-Anguiano LF. 2015. Seroepidemiology of
626 Entamoeba histolytica Infection in General Population in Rural Durango, Mexico. J Clin Med
627 Res 7:435–439.

628 4. Gilchrist CA, Petri SE, Schneider BN, Reichman DJ, Jiang N, Begum S, Watanabe K, Jansen CS,
629 Elliott KP, Burgess SL, Ma JZ, Alam M, Kabir M, Haque R, Petri WA. 2016. Role of the Gut
630 Microbiota of Children in Diarrhea Due to the Protozoan Parasite Entamoeba histolytica. J
631 Infect Dis 213:1579–1585.

632 5. Haque R, Huston CD, Hughes M, Houpt E, Petri WA. 2003. Amebiasis. New England Journal
633 of Medicine 348:1565–1573.

634 6. Petri WA, Haque R, Mann BJ. 2002. The Bittersweet Interface of Parasite and Host: Lectin-
635 Carbohydrate Interactions During Human Invasion by the Parasite Entamoeba histolytica.
636 Annu Rev Microbiol 56:39–64.

637 7. Reed SL, Curd JG, Gigli I, Gillin FD, Braude AI. 1986. Activation of complement by pathogenic
638 and nonpathogenic Entamoeba histolytica. J Immunol 136:2265–2270.

639 8. Costa CA, Nunes ÁC, Ferreira AJ, Gomes MA, Caliari MV. 2010. Entamoeba histolytica and E.
640 dispar trophozoites in the liver of hamsters: in vivo binding of antibodies and complement.
641 Parasites & Vectors 3:23.

642 9. Reed SL, Ember JA, Herdman DS, DiScipio RG, Hugli TE, Gigli I. 1995. The extracellular
643 neutral cysteine proteinase of Entamoeba histolytica degrades anaphylatoxins C3a and C5a.
644 J Immunol 155:266–274.

645 10. Reed SL, Gigli I. 1990. Lysis of complement-sensitive Entamoeba histolytica by activated
646 terminal complement components. Initiation of complement activation by an extracellular
647 neutral cysteine proteinase. J Clin Invest 86:1815–1822.

648 11. Reed SL, Keene WE, McKerrow JH, Gigli I. 1989. Cleavage of C3 by a neutral cysteine
649 proteinase of Entamoeba histolytica. J Immunol 143:189–195.

650 12. Braga LL, Ninomiya H, McCoy JJ, Eacker S, Wiedmer T, Pham C, Wood S, Sims PJ, Petri WA.
651 1992. Inhibition of the complement membrane attack complex by the galactose-specific
652 adhesion of Entamoeba histolytica. J Clin Invest 90:1131–1137.

653 13. Miller HW, Suleiman RL, Ralston KS. 2019. Trogocytosis by Entamoeba histolytica Mediates
654 Acquisition and Display of Human Cell Membrane Proteins and Evasion of Lysis by Human
655 Serum. mBio 10:e00068-19.

656 14. Bettadapur A, Miller HW, Ralston KS. 2020. Biting Off What Can Be Chewed: Trogocytosis in
657 Health, Infection, and Disease. Infect Immun 88:e00930-19.

658 15. Ralston KS, Solga MD, Mackey-Lawrence NM, Somlata null, Bhattacharya A, Petri WA.
659 2014. Trogocytosis by Entamoeba histolytica contributes to cell killing and tissue invasion.
660 Nature 508:526–530.

661 16. González-Ruiz A, Haque R, Aguirre A, Castañón G, Hall A, Guhl F, Ruiz-Palacios G, Miles MA,
662 Warhurst DC. 1994. Value of microscopy in the diagnosis of dysentery associated with
663 invasive Entamoeba histolytica. J Clin Pathol 47:236–239.

664 17. Davies A, Simmons DL, Hale G, Harrison RA, Tighe H, Lachmann PJ, Waldmann H. 1989.
665 CD59, an LY-6-like protein expressed in human lymphoid cells, regulates the action of the
666 complement membrane attack complex on homologous cells. Journal of Experimental
667 Medicine 170:637–654.

668 18. Štefanová I, Hilgert I, Krištofová H, Brown R, Low MG, Hořejši V. 1989. Characterization of a
669 broadly expressed human leucocyte surface antigen MEM-43 anchored in membrane
670 through phosphatidylinositol. Molecular Immunology 26:153–161.

671 19. Cinek T, Horejsí V. 1992. The nature of large noncovalent complexes containing glycosyl-
672 phosphatidylinositol-anchored membrane glycoproteins and protein tyrosine kinases. The
673 Journal of Immunology 149:2262–2270.

674 20. Rollins SA, Sims PJ. 1990. The complement-inhibitory activity of CD59 resides in its capacity
675 to block incorporation of C9 into membrane C5b-9. J Immunol 144:3478–3483.

676 21. Meri S, Morgan BP, Davies A, Daniels RH, Olavesen MG, Waldmann H, Lachmann PJ. 1990.
677 Human protectin (CD59), an 18,000-20,000 MW complement lysis restricting factor, inhibits
678 C5b-8 catalysed insertion of C9 into lipid bilayers. Immunology 71:1–9.

679 22. Zhao J, Rollins SA, Maher SE, Bothwell AL, Sims PJ. 1991. Amplified gene expression in
680 CD59-transfected Chinese hamster ovary cells confers protection against the membrane
681 attack complex of human complement. J Biol Chem 266:13418–13422.

682 23. Ventura-Juárez J, Campos-Rodríguez R, Jarillo-Luna RA, Muñoz-Fernández L, Escario-G-
683 Trevijano JA, Pérez-Serrano J, Quintanar JL, Salinas E, Villalobos-Gómez FR. 2009.
684 Trophozoites of Entamoeba histolytica express a CD59-like molecule in human colon.
685 Parasitol Res 104:821–826.

686 24. Wang G, Liszewski MK, Chan AC, Atkinson JP. 2000. Membrane Cofactor Protein (MCP;
687 CD46): Isoform-Specific Tyrosine Phosphorylation. The Journal of Immunology 164:1839–
688 1846.

689 25. Riley-Vargas RC, Gill DB, Kemper C, Liszewski MK, Atkinson JP. 2004. CD46: expanding
690 beyond complement regulation. Trends in Immunology 25:496–503.

691 26. Liszewski MK, Atkinson JP. 2015. Complement regulator CD46: genetic variants and disease
692 associations. Human Genomics 9:7.

693 27. Seya T, Turner JR, Atkinson JP. 1986. Purification and characterization of a membrane
694 protein (gp45-70) that is a cofactor for cleavage of C3b and C4b. J Exp Med 163:837–855.

695 28. Goslings WR, Blom DJ, de Waard-Siebinga I, van Beelen E, Claas FH, Jager MJ, Gorter A.
696 1996. Membrane-bound regulators of complement activation in uveal melanomas. CD46,
697 CD55, and CD59 in uveal melanomas. Invest Ophthalmol Vis Sci 37:1884–1891.

698 29. Varsano S, Rashkovsky L, Shapiro H, Ophir D, Mark-Bentankur T. 1998. Human lung cancer
699 cell lines express cell membrane complement inhibitory proteins and are extremely
700 resistant to complement-mediated lysis; a comparison with normal human respiratory
701 epithelium in vitro, and an insight into mechanism(s) of resistance. Clin Exp Immunol
702 113:173–182.

703 30. Nicholson-Weller A, Burge J, Fearon DT, Weller PF, Austen KF. 1982. Isolation of a human
704 erythrocyte membrane glycoprotein with decay-accelerating activity for C3 convertases of
705 the complement system. The Journal of Immunology 129:184–189.

706 31. Medof ME, Kinoshita T, Nussenzweig V. 1984. Inhibition of complement activation on the
707 surface of cells after incorporation of decay-accelerating factor (DAF) into their membranes.
708 J Exp Med 160:1558–1578.

709 32. Fishelson Z, Donin N, Zell S, Schultz S, Kirschfink M. 2003. Obstacles to cancer
710 immunotherapy: expression of membrane complement regulatory proteins (mCRPs) in
711 tumors. Molecular Immunology 40:109–123.

712 33. Gelderman KA, Blok VT, Fleuren GJ, Gorter A. 2002. The Inhibitory Effect of CD46, CD55, and
713 CD59 on Complement Activation After Immunotherapeutic Treatment of Cervical
714 Carcinoma Cells with Monoclonal Antibodies or Bispecific Monoclonal Antibodies. Lab
715 Invest 82:483–493.

716 34. Jurianz K, Maslak S, Garcia-Schüler H, Fishelson Z, Kirschfink M. 1999. Neutralization of
717 complement regulatory proteins augments lysis of breast carcinoma cells targeted with
718 rhumAb anti-HER2. Immunopharmacology 42:209–218.

719 35. Suleiman RL, Ralston KS. Growth and genetic manipulation of Entamoeba histolytica.
720 Current Protocols in Microbiology.

721 36. Cong L, Ran FA, Cox D, Lin S, Barretto R, Habib N, Hsu PD, Wu X, Jiang W, Marraffini LA,
722 Zhang F. 2013. Multiplex genome engineering using CRISPR/Cas systems. Science 339:819–
723 823.

724 37. Thielen AJF, van Baarsen IM, Jongsma ML, Zeerleder S, Spaapen RM, Wouters D. 2018.
725 CRISPR/Cas9 generated human CD46, CD55 and CD59 knockout cell lines as a tool for
726 complement research. Journal of Immunological Methods 456:15–22.

727 38. Saito-Nakano Y, Yasuda T, Nakada-Tsukui K, Leippe M, Nozaki T. 2004. Rab5-associated
728 Vacuoles Play a Unique Role in Phagocytosis of the Enteric Protozoan Parasite Entamoeba
729 histolytica*. Journal of Biological Chemistry 279:49497–49507.

730 39. Saffer LD, Petri WA. 1991. Role of the galactose lectin of Entamoeba histolytica in
731 adherence-dependent killing of mammalian cells. Infect Immun 59:4681–4683.

732 40. Schindelin J, Arganda-Carreras I, Frise E, Kaynig V, Longair M, Pietzsch T, Preibisch S, Rueden
733 C, Saalfeld S, Schmid B, Tinevez J-Y, White DJ, Hartenstein V, Eliceiri K, Tomancak P, Cardona
734 A. 2012. Fiji: an open-source platform for biological-image analysis. Nat Methods 9:676–
735 682.

736

737 **FIGURE LEGENDS**

738 **Figure 1: Ingestion of latex beads does not protect amoebae from complement lysis**

739 Amoebae were incubated with $3x10^6$ or $1.5x10^7$ fluorescent latex beads for 1 hour or were
740 incubated without latex beads, and then exposed to human serum. Amoebic viability was
741 determined with Zombie Violet viability dye. Imaging flow cytometry was used to quantify bead
742 ingestion and amoebic viability. **(A)** The percentage of amoebae that had ingested any number
743 of latex beads. **(B)** Mean number of ingested beads among amoebae that had ingested beads.
744 **(C)** Normalized amoeba death following exposure to human serum. Values are normalized to
745 the amoebae that were incubated without latex beads. **(D)** Quantification of the number of
746 ingested beads per amoeba; shown are the data plots from one replicate per sample type.
747 Amoebae that did not perform bead ingestion fall into the "Bead –" gate, while amoebae that
748 ingested beads fall into the "Bead +" gate. **(G)** Representative images of amoebae that were
749 incubated without beads, or in the presence of $3x10^6$ or $1.5x10^7$ beads. Ingested beads are
750 shown in yellow. Data are from four replicates across two independent experiments.

751 **Figure 2: Amoebic protection from complement following trogocytosis is dose-dependent.**

752 Amoebae were labeled with CMFDA cytoplasm dye and incubated in the absence of human
753 cells, or with increasing concentrations of human Jurkat cells or primary human red blood cells.
754 Human cells were labeled with DiD membrane dye. Following exposure to human serum,
755 amoeba death was assessed with Zombie Violet viability dye and ingested human cell material
756 was determined by quantifying mean fluorescence intensity (MFI) of DiD present on amoebae.
757 **(A)** Normalized MFI of DiD on amoebae incubated in the absence of Jurkat cells or with
758 increasing concentrations of Jurkat cells. **(B)** Normalized death of amoebae from conditions in

759 panel A. **(C)** Death of amoebae from conditions in panel A, expressed as percent protection.
760 Percent protection was calculated by subtracting the total death of amoebae incubated with
761 human cells from the total death of amoebae incubated in the absence of Jurkat cells. **(D)**
762 Normalized MFI of DiD on amoebae incubated in the absence of red blood cells or with
763 increasing concentrations of red blood cells. **(E)** Normalized death of amoebae from conditions
764 in panel D. **(F)** Death of amoebae from conditions in panel D, expressed as percent protection.
765 **(G)** Representative images of amoebae incubated with increasing concentrations of Jurkat cells.
766 Amoebae are shown in green and ingested human cell material is shown in red. Data were
767 analyzed by imaging flow cytometry and are from 6 replicates across 3 independent
768 experiments. **(H)** Representative images of amoebae incubated with red blood cells. Data were
769 analyzed by imaging flow cytometry and are from 6 replicates across 3 independent
770 experiments.

771 **Figure 3: Amoebic trogocytosis of human cells inhibits deposition of complement C3b.**
772 Amoebae were incubated in the absence of Jurkat T cells or in the presence of Jurkat cells, and
773 subsequently exposed to human serum. Viability was assessed with Zombie Violet dye. The
774 presence of C3b was detected using a mouse monoclonal antibody to C3b and iC3b. **(A)** Death
775 of amoebae that were incubated in the absence of Jurkat cells or in the presence of Jurkat cells.
776 **(B)** Mean fluorescence intensity of deposited C3b on amoebae. **(C)** Deposited C3b on dead or
777 live amoebae. **(D)** Deposited C3b on dead or live amoebae that had been incubated in the
778 absence of Jurkat cells (open circles) or in the presence of Jurkat cells (filled circles). **(E)**
779 Representative images of C3b deposition (red) on live or dead amoebae. Data were analyzed by
780 imaging flow cytometry and are from 6 replicates across 3 independent experiments.

781 **Figure 4: Amoebae acquire and display the complement regulatory protein CD59 from human**
782 **cells.**
783 Amoebae were allowed to perform trogocytosis on human Jurkat T cells for 5 minutes or 1
784 hour, or were incubated in the absence of Jurkat cells. Human CD59 (red) was detected on the
785 amoebae surface by monoclonal antibody staining. Amoebae were labeled with CMFDA (green)
786 and human cell nuclei were labeled with Hoechst (blue). **(A)** Representative images from
787 amoebae incubated in the absence of Jurkat cells or amoebae that performed trogocytosis on
788 human Jurkat T cells for 5 minutes or 1 hour. Arrows indicate patches of displayed CD59 on the
789 amoeba surface. **(B)** 3D rendering of Z stack images taken from amoebae that were incubated
790 with human Jurkat T cells for 1 hour. **(C)** Zoomed in image of amoebae that were incubated
791 with human Jurkat T cells for 1 hour. Data were analyzed by confocal microscopy. 136 Images
792 were collected from 1 independent experiment.
793 **Figure 5: The amount of displayed CD59 increases with increased trogocytosis of human cells.**
794 Acquired CD59 molecules were quantified on amoebae that were allowed to perform
795 trogocytosis on human Jurkat T cells for 5 minutes or 1 hour, or were incubated in the absence
796 of Jurkat cells. **(A)** Masking strategy for analysis of displayed CD59 on the amoeba surface. A
797 mask was created in order to allow for the detection of CD59 that overlapped with amoebae,
798 while excluding CD59 on intact human cells attached to amoebae. The mask is displayed in
799 turquoise, as an overlay on the individual images. Amoebae were labeled with CMFDA (green),
800 human cell nuclei were labeled with Hoechst (blue), and CD59 was detected with a monoclonal
801 antibody (red). Extracellular human cell nuclei fluorescence was removed from the masked
802 analysis area. The excluded area around human cell nuclei was then dilated by 4 pixels to

803 include the entire diameter of the intact extra-cellular human cells and associated CD59. CD59
804 was analyzed in the remaining masked analysis area of each image to allow for analysis of
805 displayed patches of acquired CD59 on amoebae. **(B)** The normalized mean fluorescence
806 intensity of CD59 on amoebae after 5 minutes or 1 hour of trogocytosis or amoebae that were
807 incubated in the absence of Jurkat cells. To normalize the data, samples were normalized to the
808 1 hour of trogocytosis condition. **(C)** Representative images of amoebae that had performed
809 trogocytosis on human Jurkat T cells for 5 minutes or 1 hour. Arrows indicate displayed CD59.
810 Data were analyzed by imaging flow cytometry and are from 5 replicates across 3 independent
811 experiments. The no primary control condition was performed in 2 of 3 independent
812 experiments and data are from 3 replicates.

813 **Figure 6: Removal of CD59 and CD46 is not sufficient to sensitize amoebae to complement**
814 **lysis.**

815 **(A-D)** Human Jurkat T cells deficient in CD59 or CD46 were constructed using CRISPR/Cas9.
816 Immunofluorescence and imaging flow cytometry were used to quantify CD59 or CD46. **(A)**
817 Representative images of CD59 antibody staining (red) in vector control human cells or CD59
818 mutants. **(B)** Intensity of CD59 antibody staining in vector control human cells (gray) or CD59
819 mutants (black). 99.5% of CD59 mutants were in the CD59-negative gate ("-CD59"), while 0.75%
820 of vector control cells were in this gate. **(C)** Representative images of CD46 antibody staining
821 (red) in vector control human cells or CD46 mutants. **(D)** Intensity of CD46 antibody staining in
822 vector control human cells (gray) or CD46 mutants (black). 99.5% of CD46 mutants were in the
823 CD46-negative gate ("-CD46"), while 0.27% of vector control cells were in this gate. **(E-F)**
824 Amoebae were labeled with CMFDA cytoplasm dye and incubated in the absence of Jurkat cells

825 or with Jurkat cells. Human cell lines were either vector control cells, CD59 KO mutants, or
826 CD46 KO mutants. Human cells were labeled with DiD membrane dye. Following exposure to
827 human serum, amoeba death was assessed with Zombie Violet viability dye and ingested
828 human cell material was determined by quantifying mean fluorescence intensity (MFI) of DiD
829 present on amoebae. **(E)** Normalized death of amoebae. **(F)** Normalized mean fluorescence
830 intensity of DiD on amoebae. Data were analyzed by imaging flow cytometry and are from 6
831 replicates across 3 independent experiments.

832 **Figure 7: Amoebae transfected with expression plasmids display human CD46 or CD55.**
833 Amoebae were transfected with expression constructs for human CD46 or human CD55, or the
834 expression plasmid backbone as a negative control. **(A)** RT-PCR analysis with primers specific for
835 human CD46, human CD55, or amoebic GAPDH. Samples were incubated with or without
836 reverse transcriptase (RT +/-), to control for DNA contamination. **(B-J)** Amoebae were labeled
837 with a cytoplasmic dye (CMFDA) and immunofluorescence was performed without
838 permeabilization. **(B)** Mean fluorescence intensity of human CD46 antibody staining. Amoebae
839 were stably transfected with a plasmid for expression of human CD46 (red) or vector backbone
840 (beige), and were stained using a CD46 primary antibody and a far red secondary antibody.
841 Amoebae expressing human CD46 were also incubated without primary antibody (grey), or
842 without any antibodies (black). **(C)** Mean fluorescence intensity of human CD55 antibody
843 staining. Amoebae were stably transfected with a plasmid for expression of human CD55 (blue)
844 or vector backbone (beige), and were stained using a CD46 primary antibody and a far red
845 secondary antibody. Amoebae expressing human CD55 were also incubated without primary
846 antibody (grey), or without any antibodies (black). **(D)** Mean fluorescence intensity of amoebic

847 Gal/GalNAc lectin antibody staining. Amoebae were stably transfected with a plasmid for
848 expression of human CD46 (red), or human CD55 (blue), or vector backbone (beige), and were
849 stained using a Gal/GalNAc lectin primary antibody and a far red secondary antibody. Amoebae
850 were also incubated without primary antibody, or without any antibodies. **(E-G)** Histograms
851 corresponding to the mean fluorescence intensity data shown in panels B-D. Panel G shows
852 antibody staining of vector control amoebae, stained with both antibodies (beige), without
853 primary antibody (grey), or without any antibodies (black). (H-J) Representative images
854 corresponding to the analysis shown in panels B-G. Data shown in panel A are representative of
855 two replicates. Data shown in panels B-J were analyzed by imaging flow cytometry are from 3-4
856 replicates across 2 independent experiments; the data from one independent experiment are
857 shown.

858 **Figure 8: Display of human CD46 or CD55 is sufficient to protect amoebae from complement**
859 **lysis.**

860 Amoebae were stably transfected with CD46 or CD55 expression constructs, or vector
861 backbone. Following exposure to either media or human serum, amoeba viability was assessed
862 using Zombie Violet viability dye and imaging flow cytometry. Amoebic death was normalized
863 to vector control amoebae that were incubated with human serum. These data are from 8
864 replicates across 4 independent experiments.

865 **TABLES**

866 **Table 1: Primers used in these studies.**

Purpose	Primer Name	F/R	Sequence
Cloning of guide RNAs into the pX330-U6-Chimeric_BB-CBh-hSpCas9 plasmid backbone	CD59 gRNA **(BbsI overhang)**	Forward	**CACC**GCAAGGAGGGTCTGTCCTGTT
	CD59 gRNA **(BbsI overhang)**	Reverse	**AAAC**AACAGGACAGACCCTCCTTGC
	CD46 gRNA **(BbsI overhang)**	Forward	**CACC**GAAAGGGACACTCGCGGCGGC
	CD46 gRNA **(BbsI overhang)**	Reverse	**AAAC**GCCGCCGCGAGTGTCCCTTTC
Sanger sequencing of CRISPR gRNA plasmids	GENEWIZ Universal Primer "U6"	Forward	GACTATCATATGCTTACCGT
BLAST-identified primer sets for specific PCR amplification of CD59 and CD46	CD59 PCR amplification	Forward	TTGACTCACTGACCCTGATGG
	CD59 PCR amplification	Reverse	TATCCATTGGTGTCCCCAAGC
	CD46 PCR amplification	Forward	ACAAATATGACGGCGAGCCA
	CD46 PCR amplification	Reverse	GGCTCAATCCCGAAAACACG
Sanger Sequencing of PCR product from CRISPR knockout clones	CD59 sequencing	Forward	GGGGCTTATAGGGACTGAGC
	CD46 sequencing	Forward	ACCTCTCGAAGGCCAAGG
Gibson cloning of CD46 and CD55 coding sequences into a pEhEx plasmid backbone	CD55 coding sequence **(homology to pEhEx)**	Forward	**AAACACATTAACAGATCTT**CATGACCGTCGCGCGGCCGAG
	CD55 coding sequence **(homology to pEhEx)**	Reverse	**GAAGAGTTCAACTCGAGTGG**CTAAGTCAGCAAGCCCATGG
	CD46 coding sequence **(homology to pEhEx)**	Forward	**AAACACATTAACAGATCTTC**ATGGAGCCTCCCGGCCGCCG
	CD46 coding sequence **(homology to pEhEx)**	Reverse	**GAAGAGTTCAACTCGAGTGG**TCAGCCTCTCTGCTCTGCTG
	pEhEx **(homology to CD46 coding sequence)**	Forward	CAGCAGAGCAGAGAGGCTGA**CCACTCGAGTTGAACTCTTC**
	pEhEx **(homology to CD46 coding sequence)**	Reverse	CGGCGGCCGGGAGGCTCCAT**GAAGATCTGTTAATGTGTTT**

Sequencing of CD59 and CD46 expression plasmids	pEhEx CS UTR Primer	Forward	TCAGTCTTACCACGTCATAAAGT
	pEhEx CS UTR Primer	Reverse	TGCAAGAAGATGTTACAAAGCA
RT-PCR of amoebae mutants	CD46 RT-PCR	Forward	TCCCTGCAAATGGGACTTAC
	CD46 RT-PCR	Reverse	GGGGGATCCCAAGTACTGTT
	CD55 RT-PCR	Forward	ATGAGTGCCGTCCAGGTTAC
	CD55 RT-PCR	Reverse	CTGAACTGTTGGTGGGACCT

867

868 **SUPPLEMENTAL MATERIAL**

869 **SUPPLEMENTAL FIGURE LEGENDS**

870 **Figure S1: Gating strategy used for analysis of bead ingestion experiments**

871 Amoebae were gated on by brightfield area and aspect ratio during acquisition. Next, using
872 Gradient RMS Bright Field, focused cells were gated on from total collected events. Because
873 amoebae remained unstained in these experiments, single amoebae were then gated on using
874 brightfield area and aspect ratio. From the single amoebae population, amoebae viability and
875 bead ingestion were measured. Dead amoebae were gated on using fluorescence intensity of
876 Zombie Violet dye and side scatter. Bead ingestion was quantified using the "spot count "
877 feature in Amnis IDEAS software and quantified spots of red bead fluorescence.

878 **Figure S2: Gating strategy used for analysis of experiments with increasing numbers of human**
879 **cells, and for immunofluorescence analysis of amoebae exogenously expressing CD46 or**
880 **CD55.**

881 **(A)** Gating strategy for experiments with increasing numbers of Jurkat cells, and for
882 immunofluorescence analysis of amoebae exogenously expressing CD46 or CD55. Focused cells
883 were gated on from total collected events, using Gradient RMS Bright Field. Single amoebae
884 were gated using area and aspect ratio of CMFDA cytoplasm dye fluorescence. Dead amoebae
885 were gated on using fluorescence intensity of Zombie Violet dye and side scatter. **(B)** Gating
886 strategy for experiments with increasing numbers of red blood cells. Only amoeba events were
887 collected for analysis and were gated on using bright field area and aspect ratio during data
888 acquisition. Focused cells were gated on from total collected events, using Gradient RMS Bright
889 Field. Single amoebae were gated using area and aspect ratio of CMFDA cytoplasm dye

890 fluorescence. Dead amoebae were gated on using fluorescence intensity of Zombie Violet dye
891 and side scatter.

892 **Figure S3: Gating strategy used for analysis of C3b deposition experiments.**

893 **(A)** Focused cells were gated on from total collected events, using Gradient RMS Bright Field.
894 Single amoebae were gated using area and aspect ratio of CMFDA cytoplasm dye fluorescence.
895 Dead amoebae were gated on using fluorescence intensity of Zombie Violet dye and side
896 scatter. **(B)** Representative histograms of C3b fluorescence intensity of all single amoeba, live
897 amoeba, or dead amoeba populations.

898 **Figure S4: Biotinylated human cell membrane proteins are detected on the surface of**
899 **amoebae prior to fixation.**

900 The surface of human Jurkat cells was biotinylated prior to incubation with amoebae. Following
901 incubation, samples were placed on ice to halt membrane turnover and fluorescently-
902 conjugated streptavidin was used to detect biotinylated proteins on the surface on both human
903 cells and amoebae (magenta) prior to fixation. DNA was labeled with DAPI nucleic acid stain
904 following fixation. Arrows indicate transferred patches of human proteins on the surface of
905 amoebae. **(A)** Amoebae and biotinylated human cells were incubated together for 2 minutes.
906 **(B)** A closeup image of an amoebae from the panel shown in A with transferred human proteins
907 on its surface. **(C)** Amoebae and human cells were incubated together for 5 minutes. Amoebic
908 autofluorescence is shown in green. **(D)** 3-D reconstruction of Z stacks taken from the data in C.
909 **(E-F)** Human cells and amoebae were incubated together for 5 minutes. Amoebae cytoplasm
910 was labeled with CMFDA dye (green), and the nuclei of cells were left unstained. Data were

911 analyzed by confocal microscopy. Images in A-F are representative of data collected from 4
912 independent experiments with incubation times of 2-5 minutes.

913 **Figure S5: Gating strategy used for analysis of CD59 displayed on amoebae after 5 minutes**
914 **and 1 hour of trogocytosis.**

915 A masking strategy was developed to quantify only fluorescence of CD59 present on the
916 amoebae, and not on extracellular human cells. **(A)** Focused cells were gated on from total
917 collected events, using Gradient RMS Bright Field. Single amoebae were gated using area and
918 aspect ratio of CMFDA cytoplasm dye fluorescence. Next, fluorescence intensity of CD59 inside
919 of the masked area was measured. **(B)** Representative images of bright field, amoeba
920 cytoplasm, human cell nuclei, and CD59 fluorescence with the masked area (turquoise) applied
921 as an overlay.

922 **Figure S6: Amoebae acquire and display the complement regulatory protein CD46 from**
923 **human cells.**

924 Amoebae were incubated in the absence of Jurkat T cells, or were allowed to perform
925 trogocytosis on human Jurkat cells for 5 minutes. Human cell nuclei were pre-labeled with
926 Hoechst (blue), and amoebae were pre-labeled with CMFDA (green). Human CD46 (red) was
927 detected on the amoebae surface by monoclonal antibody staining. (A) Representative images
928 from amoebae that were incubated in the absence of Jurkat cells. (B) Representative images of
929 amoebae that performed trogocytosis on human Jurkat cells for 5 minutes. Arrows indicate
930 patches of displayed CD46 on the amoeba surface. Data were analyzed by imaging flow
931 cytometry and are from 2 replicates and 1 independent experiment.

932 **Figure S7: Removal of GPI-anchored surface proteins using phosphatidylinositol-specific**
933 **phospholipase C.**
934 Amoebae were labeled with CMFDA cytoplasm dye and incubated in the absence of Jurkat cells
935 or with Jurkat cells. Human cells were labeled with DiD membrane dye. Samples were then
936 treated with phosphatidylinositol-specific phospholipase C (PI-PLC) to remove GPI-anchored
937 proteins, or heat-inactivated phosphatidylinositol-specific phospholipase C (HI-PI-PLC) as a
938 control. Following exposure to human serum, amoeba death was assessed with Zombie Violet
939 viability dye and ingested human cell material was determined by quantifying mean
940 fluorescence intensity (MFI) of DiD present on amoebae. **(A)** Normalized death of amoebae. **(B)**
941 Normalized mean fluorescence intensity of DiD on amoebae. Data were analyzed by imaging
942 flow cytometry and are from 8 replicates across 4 independent experiments. The untreated
943 control condition was performed 3 of 4 independent experiments and data are from 6
944 replicates.
945 **Figure S8: Gating strategy used for analysis of experiments with CRISPR knockout mutants, PI-**
946 **PLC treatment experiments, amoebae exogenously expressing CD46 or CD55.**
947 Only cell events were collected for analysis (to minimize collection of debris) and were gated on
948 using bright field area and aspect ratio during data acquisition. Focused cells were gated on
949 from total collected events, using Gradient RMS Bright Field. Single amoebae were gated using
950 intensity of and aspect ratio of CMFDA cytoplasm dye fluorescence. **(A)** In CRISPR knockout
951 mutant and PI-PLC treatment experiments, amoebae were gated on a second time using
952 CMFDA fluorescence intensity and side scatter to eliminate remaining clumps of human cells
953 from the analysis. **(B)** In experiments with amoebae exogenously expressing CD46 or CD55, the

954 second amoebae gate was not used. Finally, dead amoebae were gated on using fluorescence

955 intensity of Zombie Violet dye and side scatter.

956 **Figure S9: Sequencing analysis of Jurkat CRISPR/Cas9 mutants.**

957 Chromatograms from Sanger sequencing analysis of Jurkat T cell CRISPR/Cas9 mutants.

958 Chromatograms from CD59 mutants **(A)** and CD46 mutants **(B)** show that the gene sequence of

959 the mutants is different from the vector control cells downstream of the gRNA/PAM sites.

Fig. 1

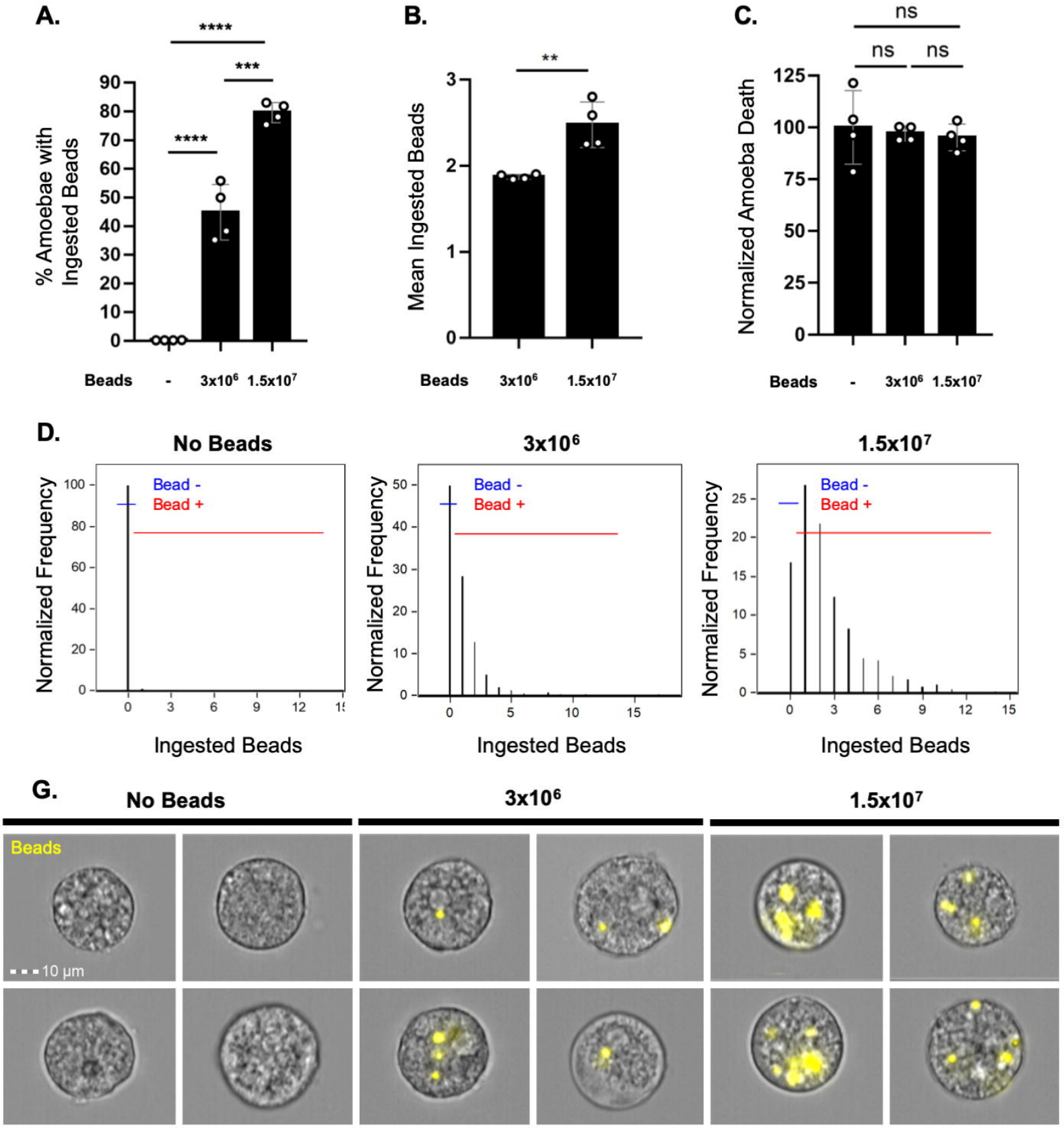
A.
****
***
****
% Amoebae with Ingested Beads
90
80
70
60
50
40
30
20
10
0
Beads
-
3x10⁶
1.5x10⁷
B.
**
Mean Ingested Beads
3
2
1
0
Beads
3x10⁶
1.5x10⁷
C.
ns
ns
ns
Normalized Amoeba Death
125
100
75
50
25
0
Beads
-
3x10⁶
1.5x10⁷
D.
No Beads
3x10⁶
1.5x10⁷
Bead -
Bead +
Normalized Frequency
Ingested Beads
G.
No Beads
3x10⁶
1.5x10⁷
Beads
10 µm

Fig. 2

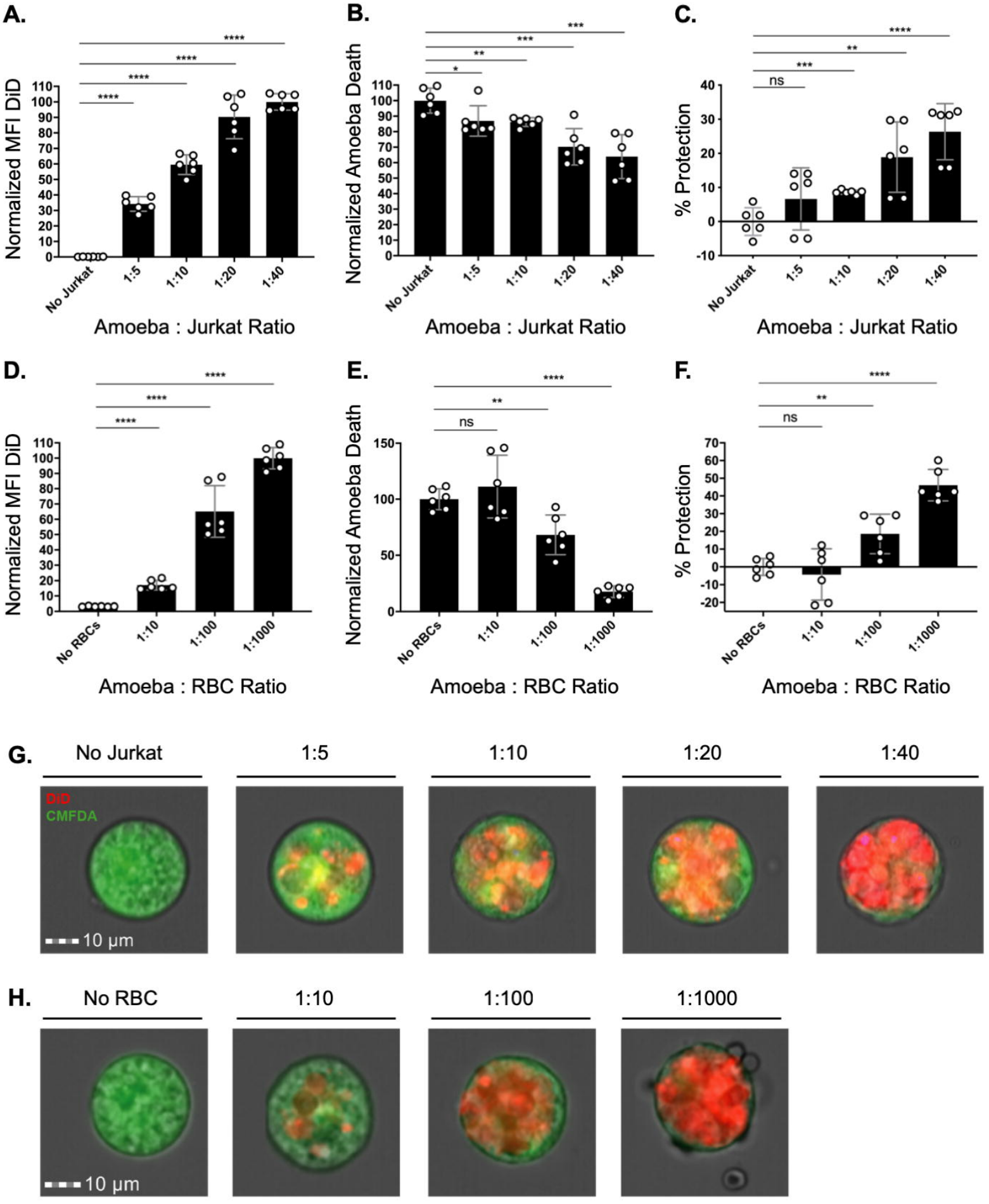
A.
Normalized MFI DiD
No Jurkat
1:5
1:10
1:20
1:40
Amoeba : Jurkat Ratio
B.
Normalized Amoeba Death
Amoeba : Jurkat Ratio
C.
% Protection
ns
Amoeba : Jurkat Ratio
D.
Normalized MFI DiD
No RBCs
1:10
1:100
1:1000
Amoeba : RBC Ratio
E.
Normalized Amoeba Death
ns
Amoeba : RBC Ratio
F.
% Protection
ns
Amoeba : RBC Ratio
G.
No Jurkat
1:5
1:10
1:20
1:40
DiD
CMFDA
10 µm
H.
No RBC
1:10
1:100
1:1000
10 µm

Fig. 3

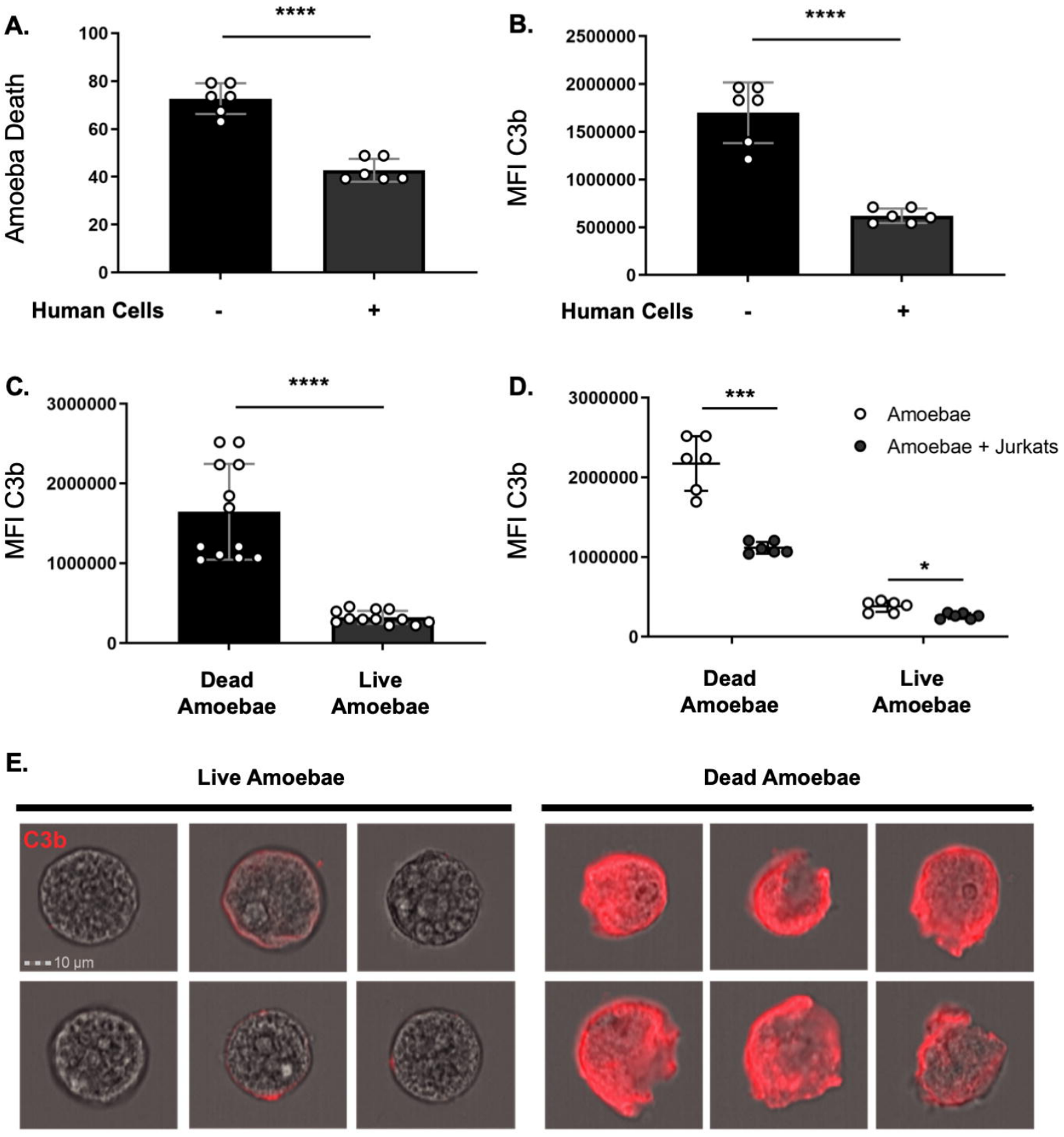
A.
****
Amoeba Death
100
80
60
40
20
0
Human Cells
-
+
B.
****
MFI C3b
2500000
2000000
1500000
1000000
500000
0
Human Cells
-
+
C.
****
MFI C3b
3000000
2000000
1000000
0
Dead Amoebae
Live Amoebae
D.
***
*
MFI C3b
3000000
2000000
1000000
0
Amoebae
Amoebae + Jurkats
Dead Amoebae
Live Amoebae
E.
Live Amoebae
Dead Amoebae
C3b
10 µm

Fig. 4

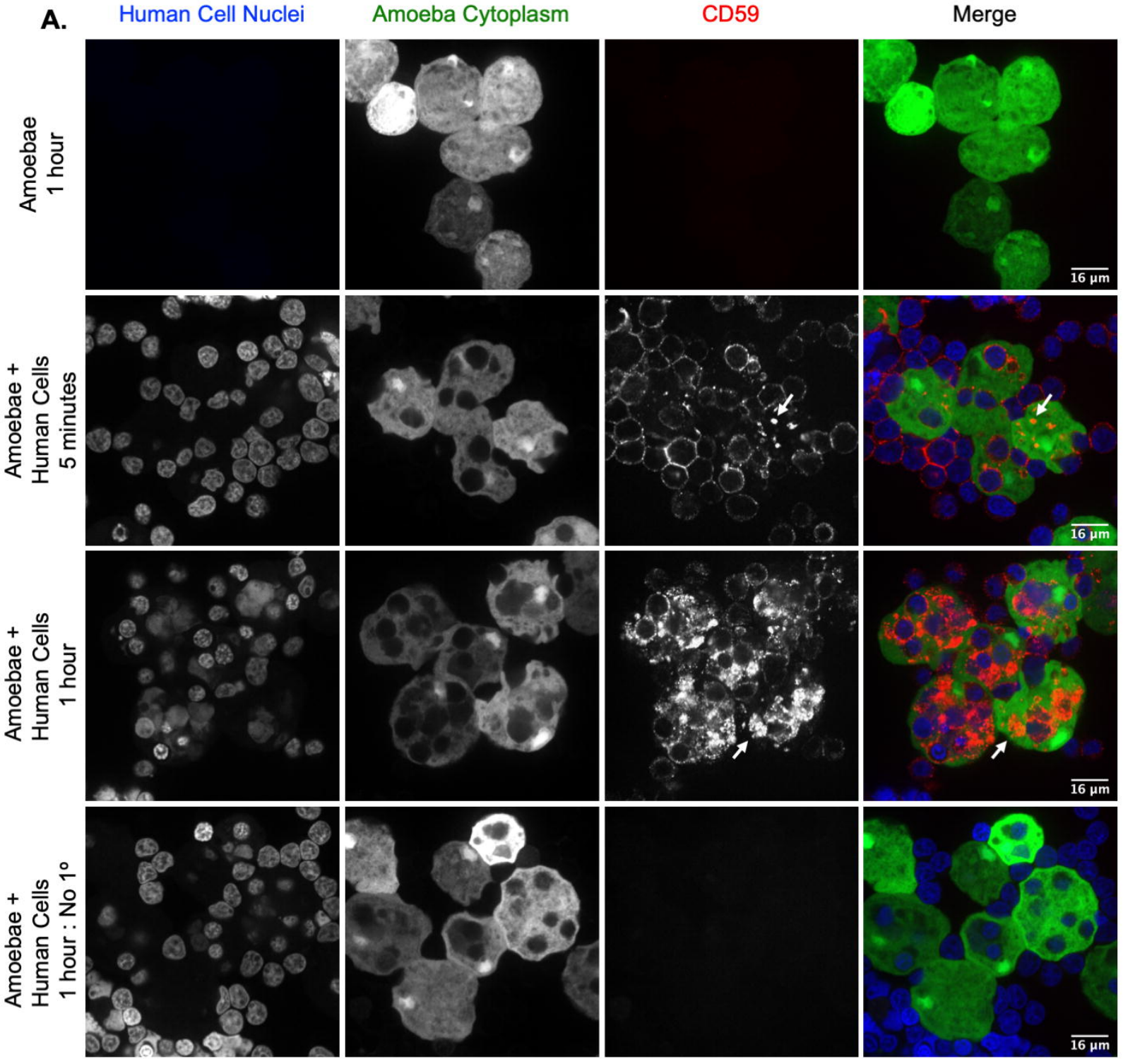
A.
Human Cell Nuclei
Amoeba Cytoplasm
CD59
Merge
Amoebae 1 hour
Amoebae + Human Cells 5 minutes
Amoebae + Human Cells 1 hour
Amoebae + Human Cells 1 hour : No 1°
16 µm

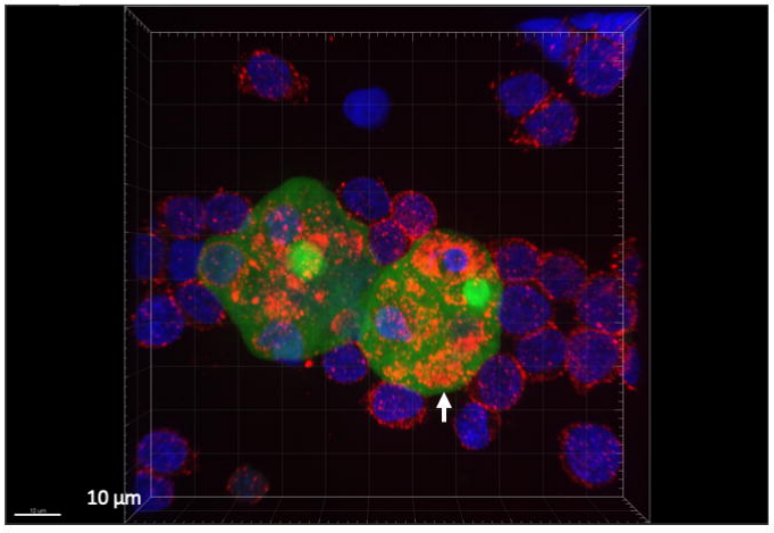
B.
10 µm

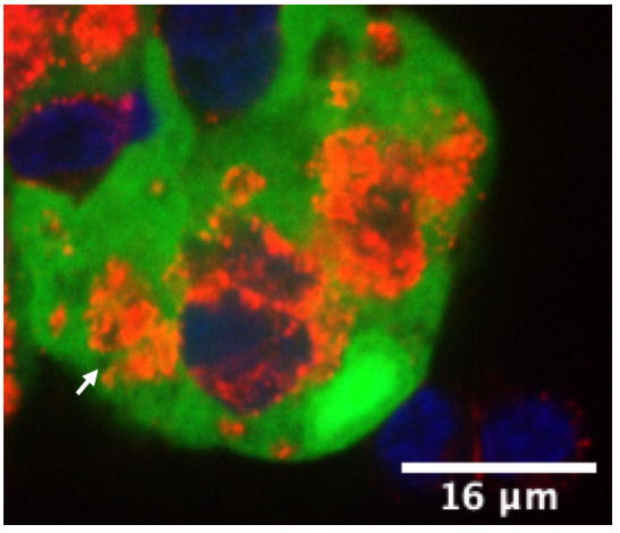
C.
16 µm

Fig. 5

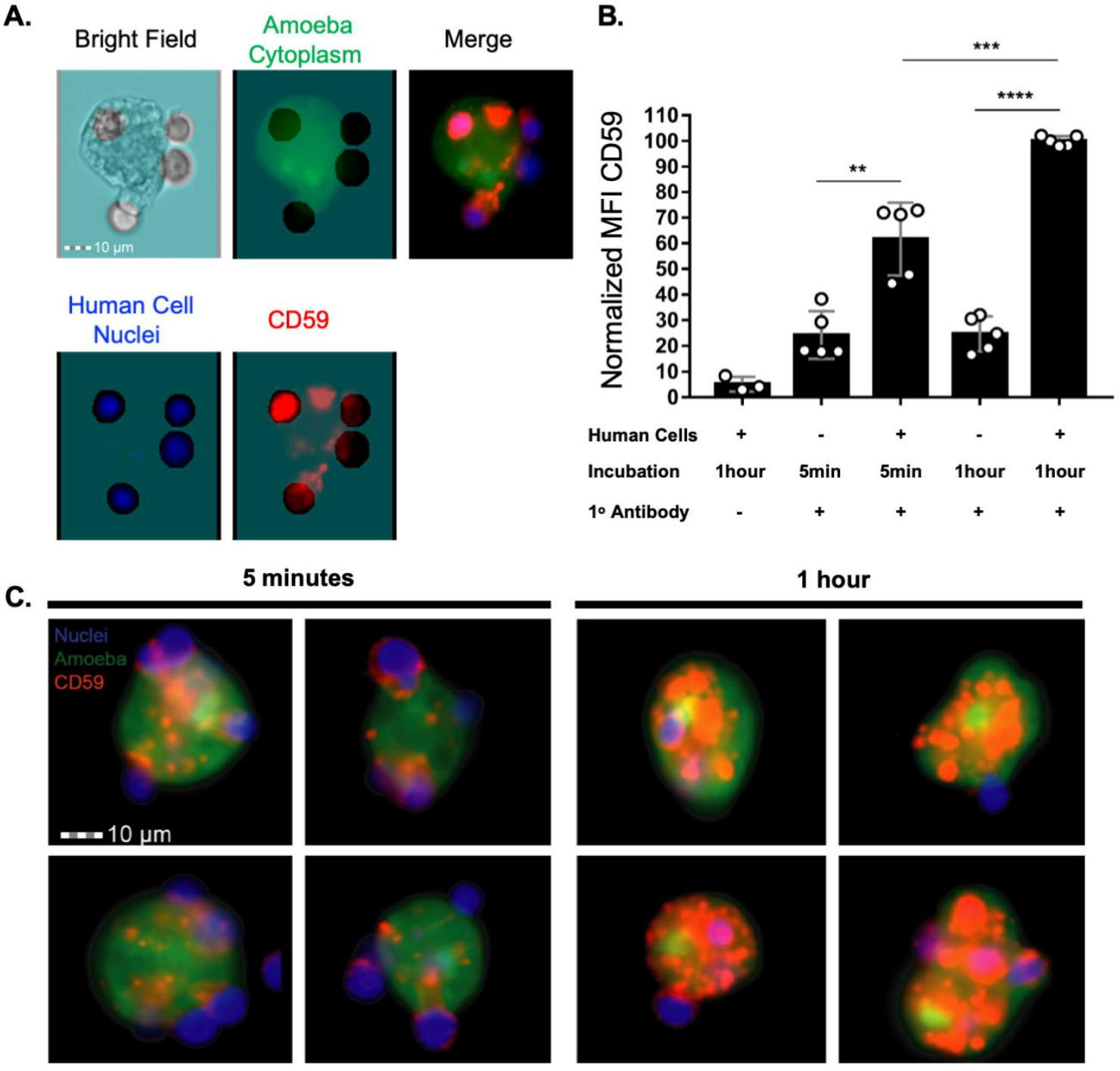
A.
Bright Field
Amoeba Cytoplasm
Merge
10 µm
Human Cell Nuclei
CD59
B.
Normalized MFI CD59
110
100
90
80
70
60
50
40
30
20
10
0
**
***
****
Human Cells + - + - +
Incubation 1hour 5min 5min 1hour 1hour
1° Antibody - + + + +
C.
5 minutes
1 hour
Nuclei
Amoeba
CD59
10 µm

Fig. 6

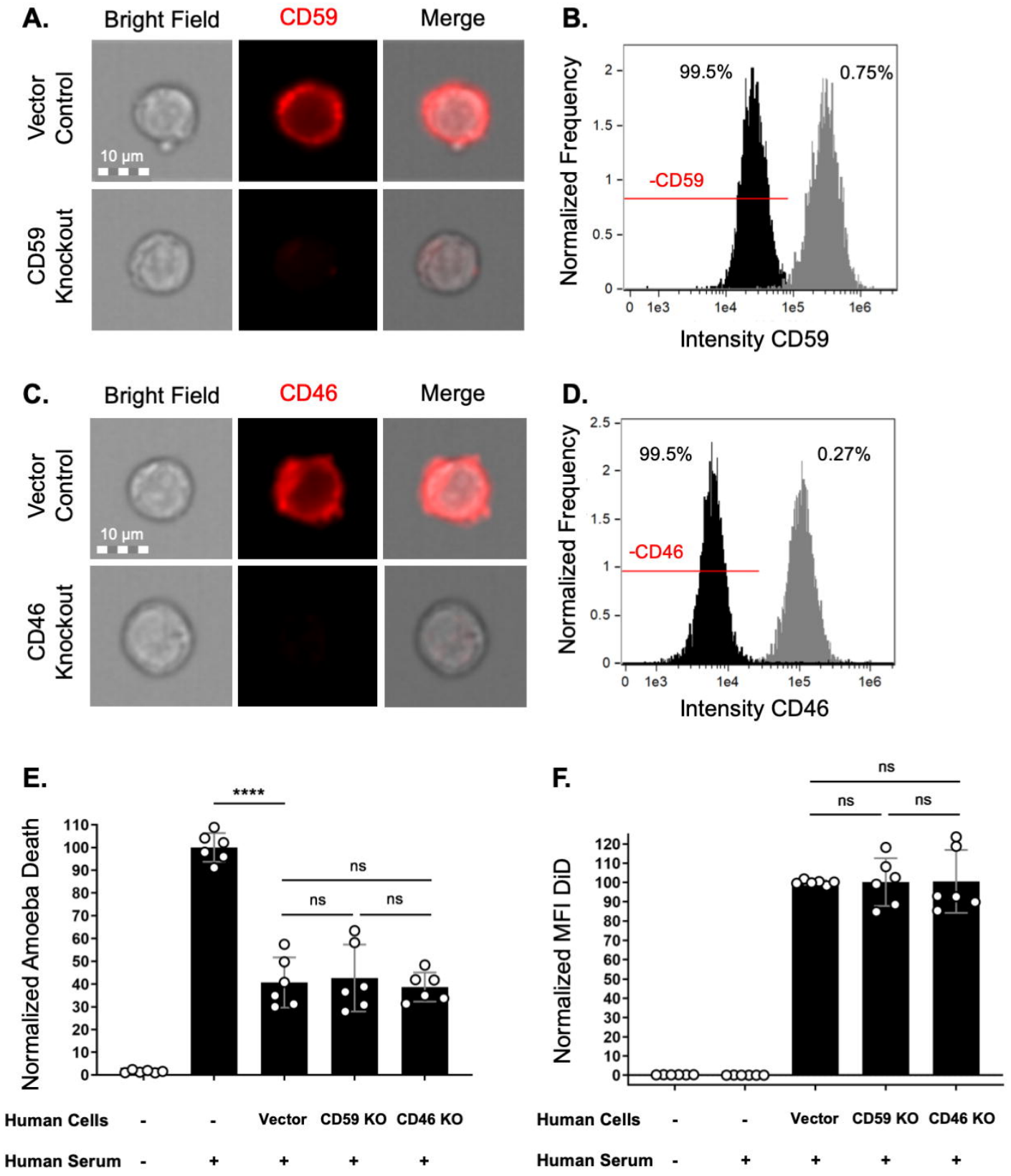
A.
Bright Field
CD59
Merge
Vector Control
CD59 Knockout
10 µm
B.
99.5%
0.75%
-CD59
Normalized Frequency
Intensity CD59
C.
Bright Field
CD46
Merge
Vector Control
CD46 Knockout
10 µm
D.
99.5%
0.27%
-CD46
Normalized Frequency
Intensity CD46
E.
****
ns
ns
ns
Normalized Amoeba Death
Human Cells - - Vector CD59 KO CD46 KO
Human Serum - + + + +
F.
ns
ns
ns
Normalized MFI DiD
Human Cells - - Vector CD59 KO CD46 KO
Human Serum - + + + +

Fig. 7

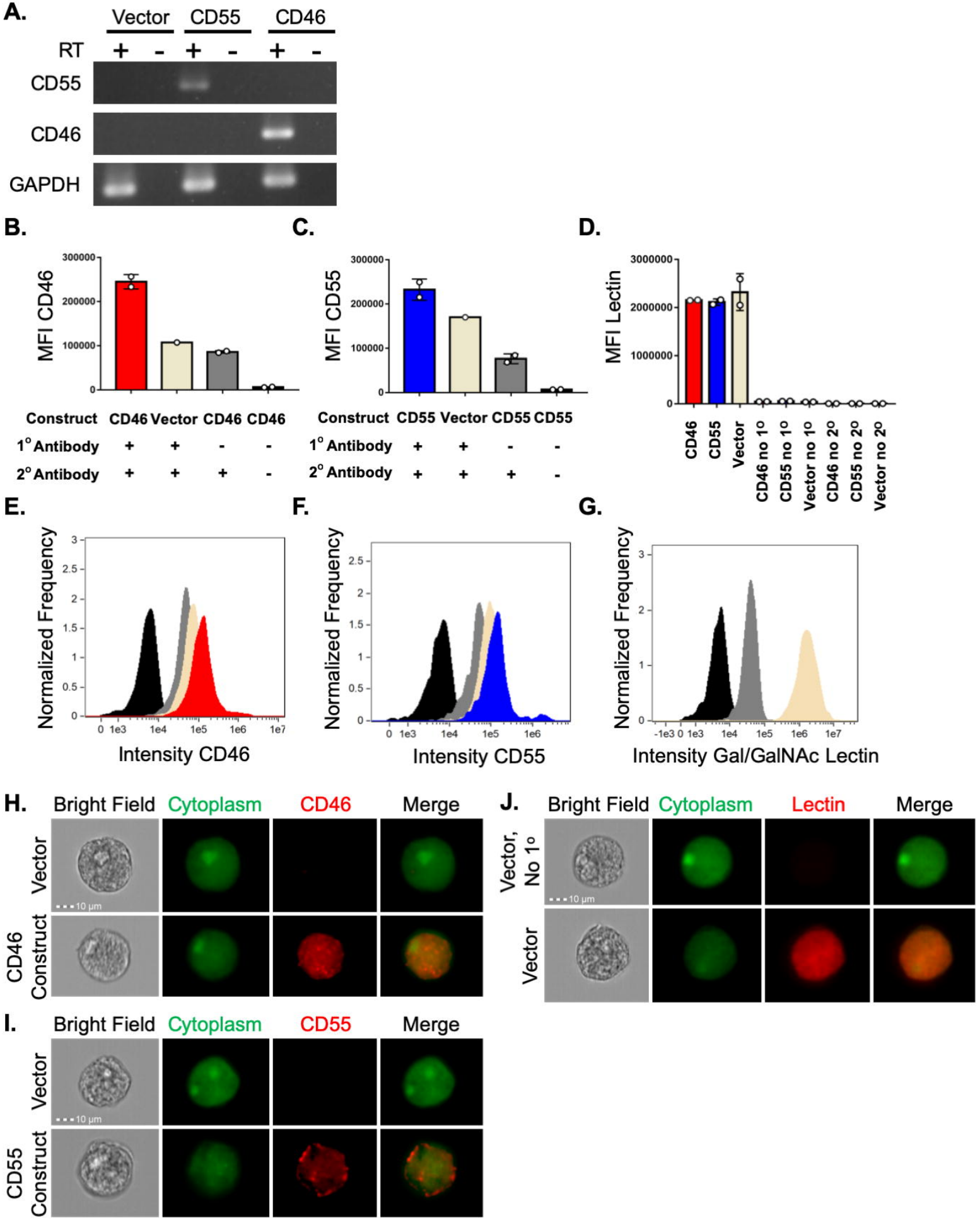
A.
Vector
CD55
CD46
RT
+ - + - + -
CD55
CD46
GAPDH
B.
MFI CD46
300000
200000
100000
0
Construct CD46 Vector CD46 CD46
1° Antibody + + - -
2° Antibody + + + -
C.
MFI CD55
300000
200000
100000
0
Construct CD55 Vector CD55 CD55
1° Antibody + + - -
2° Antibody + + + -
D.
MFI Lectin
3000000
2000000
1000000
0
CD46
CD55
Vector
CD46 no 1°
CD55 no 1°
Vector no 1°
CD46 no 2°
CD55 no 2°
Vector no 2°
E.
Normalized Frequency
Intensity CD46
F.
Normalized Frequency
Intensity CD55
G.
Normalized Frequency
Intensity Gal/GalNAc Lectin
H.
Bright Field
Cytoplasm
CD46
Merge
Vector
CD46 Construct
10 µm
J.
Bright Field
Cytoplasm
Lectin
Merge
Vector, No 1°
Vector
10 µm
I.
Bright Field
Cytoplasm
CD55
Merge
Vector
CD55 Construct
10 µm

Fig. 8

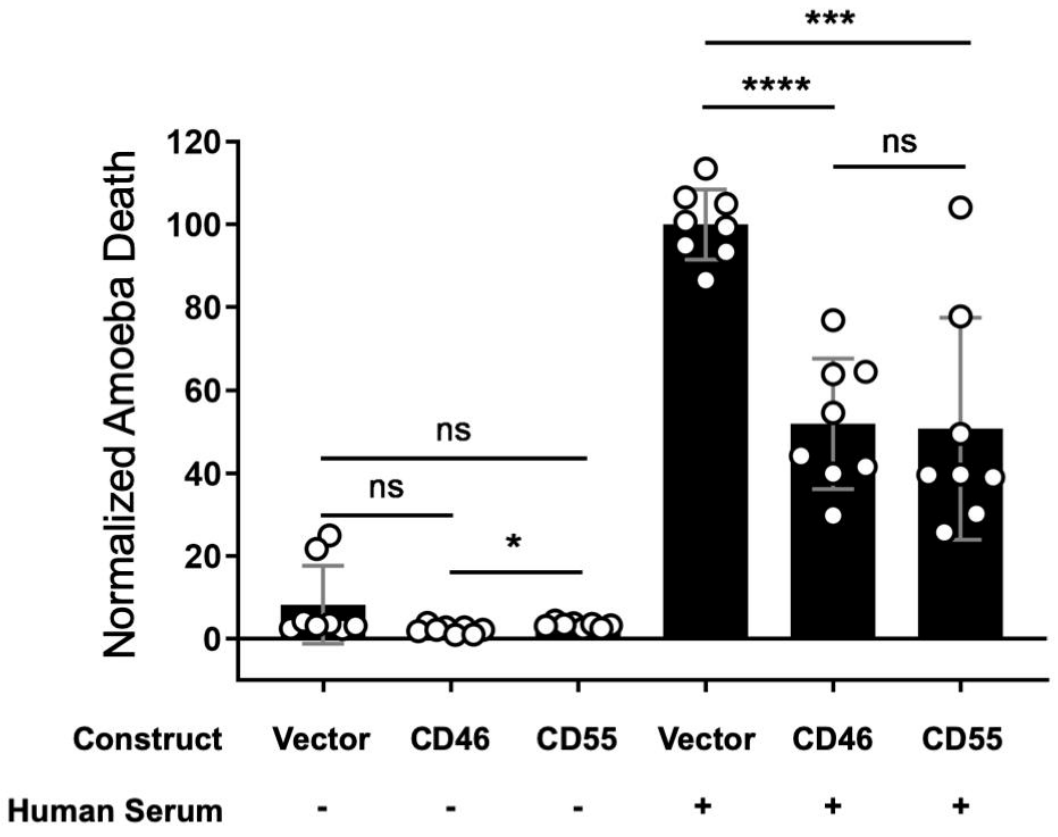
***
****
ns
ns
ns
*
Normalized Amoeba Death
120
100
80
60
40
20
0
Construct
Vector
CD46
CD55
Vector
CD46
CD55
Human Serum
-
-
-
+
+
+